UNIVERSIDAD DE INVESTIGACIÓN DE TECNOLOGÍA EXPERIMENTAL YACHAY TECH

Escuela de Ciencias Químicas e Ingeniería

TÍTULO: Synthesis and characterization of natural adsorbents derived of chitosan, Ecuadorian clay and diatomite for Ni $^{2+}$ removal from aqueous media

Trabajo de integración curricular presentado como requisito para la obtención del título de Química

Autor:

Clara Johana Carrera Marmolejo

Tutor:

PhD. Ernesto Bastardo - González

Urcuquí, Julio 2020

SECRETARÍA GENERAL
(Vicerrectorado Académico/Cancillería)
ESCUELA DE CIENCIAS QUÍMICAS E INGENIERÍA
CARRERA DE QUÍMICA
ACTA DE DEFENSA No. UITEY-CHE-2020-00041-AD

A los 17 días del mes de julio de 2020, a las 10:00 horas, de manera virtual mediante videoconferencia, y ante el Tribunal Calificador, integrado por los docentes:

Presidente Tribunal de Defensa	Dr. CAETANO SOUSA MANUEL , Ph.D.
Miembro No Tutor	Dra. LOPEZ GONZALEZ, FLORALBA AGGENY , Ph.D.
Tutor	Dr. BASTARDO GONZÁLEZ, ERNESTO LUIS , Ph.D.

El(la) señor(ita) estudiante **CARRERA MARMOLEJO, CLARA JOHANA**, con cédula de identidad No. **2350087488**, de la **ESCUELA DE CIENCIAS QUÍMICAS E INGENIERÍA**, de la Carrera de **QUÍMICA**, aprobada por el Consejo de Educación Superior (CES), mediante Resolución **RPC-SO-39-No.456-2014**, realiza a través de videoconferencia, la sustentación de su trabajo de titulación denominado: **Synthesis and characterization of natural adsorbents derived of chitosan Ecuadorian clay and diatomite for Ni2+ removal from aqueous media**, previa a la obtención del título de **QUÍMICO/A**.

El citado trabajo de titulación, fue debidamente aprobado por el(los) docente(s):

Tutor	Dr. BASTARDO GONZÁLEZ, ERNESTO LUIS , Ph.D.

Y recibió las observaciones de los otros miembros del Tribunal Calificador, las mismas que han sido incorporadas por el(la) estudiante.

Previamente cumplidos los requisitos legales y reglamentarios, el trabajo de titulación fue sustentado por el(la) estudiante y examinado por los miembros del Tribunal Calificador. Escuchada la sustentación del trabajo de titulación a través de videoconferencia, que integró la exposición de el(la) estudiante sobre el contenido de la misma y las preguntas formuladas por los miembros del Tribunal, se califica la sustentación del trabajo de titulación con las siguientes calificaciones:

Tipo	Docente	Calificación
Miembro Tribunal De Defensa	Dra. LOPEZ GONZALEZ, FLORALBA AGGENY , Ph.D.	10,0
Presidente Tribunal De Defensa	Dr. CAETANO SOUSA MANUEL , Ph.D.	9,8
Tutor	Dr. BASTARDO GONZÁLEZ, ERNESTO LUIS , Ph.D.	10,0

Lo que da un promedio de: **9.9 (Nueve punto Nueve)**, sobre 10 (diez), equivalente a: **APROBADO**

Para constancia de lo actuado, firman los miembros del Tribunal Calificador, el/la estudiante y el/la secretario ad-hoc.

Certifico que *en cumplimiento del Decreto Ejecutivo 1017 de 16 de marzo de 2020, la defensa de trabajo de titulación (o examen de grado modalidad teórico práctica) se realizó vía virtual, por lo que las firmas de los miembros del Tribunal de Defensa de Grado, constan en forma digital.*

CARRERA MARMOLEJO, CLARA JOHANA
Estudiante

MANUEL CAETANO SOUSA
Digitally signed by MANUEL CAETANO SOUSA
Date: 2020.07.17 14:22:57 -05'00'

Dr. CAETANO SOUSA MANUEL , Ph.D.
Presidente Tribunal de Defensa

ERNESTO LUIS
BASTARDO
GONZALEZ

Dr. BASTARDO GONZÁLEZ, ERNESTO LUIS , Ph.D.
Tutor

FLORALBA AGGENY LOPEZ
GONZALEZ

Dra. LOPEZ GONZALEZ, FLORALBA AGGENY , Ph.D.
Miembro No Tutor

ESCOBAR LANDAZURI, ANA MARIA
Secretario Ad-hoc

AUTORÍA

Yo, **CLARA JOHANA CARRERA MARMOLEJO,** con cédula de identidad 2350087488, declaro que las ideas, juicios, valoraciones, interpretaciones, consultas bibliográficas, definiciones y conceptualizaciones expuestas en el presente trabajo; así cómo, los procedimientos y herramientas utilizadas en la investigación, son de absoluta responsabilidad de el/la autora (a) del trabajo de integración curricular. Así mismo, me acojo a los reglamentos internos de la Universidad de Investigación de Tecnología Experimental Yachay.

Urcuquí, Julio 2020

Clara Johana Carrera Marmolejo

CI: 2350087488

AUTORIZACIÓN DE PUBLICACIÓN

Yo, **CLARA JOHANA CARRERA MARMOLEJO,** con cédula de identidad 2350087488, cedo a la Universidad de Investigación de Tecnología Experimental Yachay, los derechos de publicación de la presente obra, sin que deba haber un reconocimiento económico por este concepto. Declaro además que el texto del presente trabajo de titulación no podrá ser cedido a ninguna empresa editorial para su publicación u otros fines, sin contar previamente con la autorización escrita de la Universidad.

Asimismo, autorizo a la Universidad que realice la digitalización y publicación de este trabajo de integración curricular en el repositorio virtual, de conformidad a lo dispuesto en el Art. 144 de la Ley Orgánica de Educación Superior.

Urcuquí, Julio 2020.

Clara Johana Carrera Marmolejo

CI: 2350087488

To my lovely parents who always support me, I love you

Clara Johana Carrera Marmolejo

Acknowledgements

First, to God, for being with me every step I take.

To my parents, Mary & Alfonso, for its love, constant encouragement and guidance. I am fortunate enough to have them.

To my siblings Eliana, Alfonso, Pedro and Jodie, for making my days happier. My life would not be the same without you guys.

To my grandmother Clarita, for always believe in me.

To Gustavo, who I consider a brother, thanks for your love and advice.

To Lis, Cynthia, Jorge and Bryan for always being by my side. You guys were the best part of college.

I would like to express my gratitude to my tutor Ernesto Bastardo, PhD, for his invaluable guidance.

To professor Jose Angel Rivera, who gave me the golden opportunity to do this wonderful project on the topic.

I would like to extend my special thanks to professors Manuel & Lola, for being always ready to help with the love that characterizes them.

To professor Kamil, for advising me not to give up.

I would like to express my gratitude to researchers at CUVyTT-BUAP (Centro Universitario de Investigación y transferencia tecnológica de la Benemerita Universidad Autónoma de Puebla) which also helped me during research, specially to the director of the center Efrain Rubio, who always made me feel at home.

To all staff in laboratory, for their timely support.

Clara Johana Carrera Marmolejo

Resumen

Se prepararon adsorbentes para la eliminación efectiva de Ni^{2+} de sistemas acuosos por dispersión de quitosano en materiales locales (arcilla montmorillonita y tierras diatomeas). Los adsorbentes se sintetizaron en forma esférica usando el método de gota a gota, y fueron denotados arcilla montmorillonita natural (M), tierras diatomeas (D) y sus compositos con quitosano: arcilla de montmorillonita / quitosano (CM), tierra de diatomeas / quitosano (CD) y arcilla de montmorillonita / tierra de diatomeas / quitosano. (CMD). La composición química de los adsorbentes, la morfología de la microestructura y estructura cristalina se investigaron mediante diferentes técnicas de caracterización: espectroscopía de rayos X dispersiva (EDS), microscopía electrónica de barrido (SEM), difracción de rayos X, espectroscopía infrarroja (IR) y propiedades de textura por el modelo de Brunauer-Emmett-Teller (BET). Técnicas de adsorción Batch fueron desarrolladas para evaluar la idoneidad de los adsorbentes sintetizados y para examinar el impacto de los parámetros como el pH de la solución, la concentración inicial de metal y el tiempo de contacto en la adsorción de Ni^{2+}. En condiciones óptimas, las capacidades máximas de adsorción de los adsorbentes basados en el modelo de isoterma de Langmuir fueron 5.82, 1.66, 5.95, 8.64 y 6.95 mg/g para M, D, CM, CD y CMD, respectivamente.

Palabras clave: Arcilla montmorillonite, quitosano, adsorción, isoterma de Langmuir

Abstract

Adsorbents for an effective removal of Ni^{2+} from aqueous systems were prepared by dispersion of chitosan onto local natural materials (montmorillonite clay and diatomaceous earth). The adsorbents were synthesized into a spherical shape using the dropwise method, and they were denoted as natural montmorillonite clay (M), diatomaceous earth (D) and its composites with chitosan: montmorillonite clay/chitosan (CM), diatomaceous earth/chitosan (CD) and montmorillonite clay/diatomaceous earth/chitosan (CMD). Adsorbent's chemical composition, microstructure morphology, and crystalline structure were investigated by different characterization techniques: dispersive X-ray spectroscopy (EDS), scanning electron microscopy (SEM), X-ray diffraction, infrared spectroscopy (IR), and textural properties by the Brunauer-Emmett-Teller model. Batch adsorption studies were developed to evaluate the potential suitability of the adsorbents and to examine the impact of adsorption parameters such as solution-pH, initial metal concentration, and contact time on the Ni^{2+} adsorption. Under optimal conditions, the maximal adsorption capacities of adsorbents based on the Langmuir isotherm model were 5.82, 1.66, 5.95, 8.64 and 6.95 mg/g for M, D, CM, CD and CMD, respectively.

Keywords: Montmorillonite clay, chitosan, adsorption, Langmuir isotherm model

Table of Contents

List of Figures

List of Tables

List of Abbreviations

M: Natural montmorillonite clay
D: Natural diatomaceous earth
CM: Montmorillonite clay/Chitosan composite
CD: Natural diatomaceous earth /Chitosan composite
CMD: Montmorillonite clay//Natural diatomaceous earth/Chitosan composite

Chapter 1: Introduction

This chapter outlines the problem statement (section **¡Error! No se encuentra el origen de la referencia.**), the purpose (section 1.2), the general and specific objectives of the study (section 1.3). Finally, section 1.4 includes an outline of the remaining chapters of the thesis.

1.1 PROBLEM STATEMENT

Clean fresh water resources are scarce. One of the most challenging problems that the environment and society have to face today is the pollution of freshwater resources resulting from the improper disposal of industrial wastes. Industrial wastes contain different types of contaminants, heavy metals are one of the most concerning [1]. Toxic metals are often discharged by different industrial processes to water bodies and this can lead, in turn, to the contamination of freshwater [2]. Heavy metals are among the most dangerous pollutants impacting water resources. Due to its high toxicity, these pollutants represent a significant risk to human health, animals and the environment. In particular, Ni^{2+} is a strong skin and respiratory sensitizer and a recognized carcinogen [3]. This metal ion is highly present in industrial wastes. In Ecuador, oil refineries and local industries are important sources of emission of nickel pollutant [4]. Populations residing close to oil refineries and industries are at potential risk.

1.2 PURPOSE

To find an effective method to remove metal ion Ni^{2+} from contaminated water, in order to achieve the allowed limit by national and international organisms avoiding poisoning of living beings and thus preserving its life quality [5].

Evaluating and deepening the knowledge of alternatives that have already shown favorable preliminary results towards the sorption of metals, such as chitosan, diatomaceous earth and montmorillonite clay. These materials are naturally abundant which make them less expensive. Mineral deposits of montmorillonite clay and diatomaceous earth can be found in Guayllabamba, Ecuador. The synergy between these materials taken from different parts of the world has shown an improvement in the adsorption process [6].Then, the adsorption capacity of local adsorbents and their

synergetic effects can be used as an alternative of new low-cost materials to remove contaminants to solve the problem of availability of water quality not only in Ecuador but throughout the world. This proposal provides solutions to the aforementioned problem.

1.3 OBJECTIVES

1.3.1 General objective

The aim of this work is to Study the adsorption of metal ion Ni2+ from aqueous media using natural adsorbents: Ecuadorian montmorillonite clay, diatomaceous earth and chitosan, which are considered environmentally safe and low-cost. Also, to study synergistic effect between these adsorbents.

1.3.2 Specific objectives

- Characterize Ecuadorian montmorillonite clay and diatomaceous earth

- Study the adsorption capacity of local natural adsorbents: montmorillonite clay and diatomaceous earth.

- Synthesize composites based on adsorbents of natural origin to study their synergetic effect.

- Study the adsorption capacity of synthesized composites.

- Determine the optimal conditions (solution pH, contact time and adsorbate concentration) to favour the interaction between metal ion Ni^{2+} and adsorbents (natural adsorbents and synthesized composites).

1.4 THESIS OUTLINE

The next chapters contain a literature review (Chapter 2), the methodology of research (Chapter 3), results and discussion are shown in Chapter 4, conclusions of the thesis are presented in Chapter 5 and finally, recommendations for future works are presented in Chapter 6.

Chapter 2: Literature Review.

This chapter outlines topics concerning to water and its quality (section 2.1), the basis of adsorption and ion exchange (section 2.2), general information about adsorbents used in this study (section 2.3), section 2.4 describes adsorption isotherms models. Finally, section 2.5 describes the different characterization techniques used to elucidate adsorbents prepared (natural and composites).

2.1 WATER

Due to its vital importance, water is one of the most studied substances on planet Earth. Water is a molecule that consists of two hydrogen atoms attached to an oxygen atom. At first sight, it can be thought as a simple molecule, but the hydrogen bonds between water molecules give it complex properties that make it essential for most of carbon-based life [7]. The main properties of water are its polarity, cohesion, adhesion, surface tension, high specific heat capacity, and evaporative cooling [8]. A lot of vital functions that are carried out in different organisms depends on water extraordinary properties. For example, the high specific heat capacity of water contribute to thermal regulation and prevent local temperature fluctuations in certain organisms [9].

2.1.1 Water distribution

Water is divided mainly into two groups: fresh water and sea water. Water is unevenly distributed on the Earth's surface, 97% is present in the ocean, that is, sea water and only 3% is fresh water. The quantity of fresh water on Earth is limited and most resides in glaciers (69%), underground (30%), and to a lesser extent in lakes, rivers, and swamps (1%). As regards freshwater, not all is suitable for living beings consumption, just 1% of its total amount is usable by humans and 99% of this quantity is found underground [10].

2.1.2 Water pollution

Water quality can be compromised by the presence of different contamination agents. Contamination agents enter in water bodies due to water dissolving capacity and the release of waste in it. Water is known as an "universal solvent", its polarity give it a huge capacity of dissolving a broad type of substances (more than any other

liquid on earth) [11]. This characteristic and the lack of norms that regulates the treatment of waste before litter it, make water very vulnerable to pollution. Polluted water can be used as nutrient source by plants and living organisms in most aquatic ecosystems. Then, these plants and living organisms absorb harmful substances present in polluted water, which are passed through the food chain to consumer animals and humans. People, plants and animals who consume it can be harmed [12].

Taking into account the contaminant agent, water pollution can be classified in three main categories: pathogens pollutants, organic and inorganic pollutants [13]. Pathogens pollutants are those microorganisms such as bacteria, fungi and some viruses. *E. coli* bacteria is a good example of a commonly microorganism found in water; its presence indicates animal or human waste contamination. This kind of waste may contain organisms responsible of many types of diseases. Organic compounds pollutants are substances based on carbon, volatile organic chemicals and macro pollutants are the most common contaminants in this category. Methyl tert-butyl ether (MTBE) is a commonly detected volatile organic chemical. It has been determined that MTBE presence causes diseases like leukemia and lymphoma. Macroscopic pollutants are, as its name suggest, big objects in water bodies. Plastic waste is the most common macroscopic pollutant. Inorganic materials are related mainly to heavy metals which even in very small concentrations are harmful for living beings when are present in water bodies causing health problems which can lead to death [13]. Heavy metals present in water bodies for human consumption is one of the major concerns in public health due to its adverse effects in living organisms.

2.1.3 Heavy metals water pollution

Heavy metals is the name attributed to metals and metalloid elements that shows density larger than 5 g/cm^3 and atomic number over 20 [14]. Heavy metals are natural components of the Earth crust that can't be degraded (neither chemically nor biologically). They can be present in water with different chemical forms such as oxides or carbonates. They tend to accumulate in biological systems through different paths such as unsafe drinking water sources, ingestion of contaminated food, inhalation of polluted air and consumption of topical products [1]. Heavy metals are among the most common pollutants found in wastewater. They end in water bodies

mainly due to industrial and agricultural production, consumerist lifestyle and also from soil breaking by, for example, acidic rain [1].

The industrial sector uses large volumes of water and, as a result, produces considerable amounts of sewage discharge containing pollutants. Currently, the industry is considered to be one of the most polluting, in spite of numerous attempts over the past 30 years to clean up its disposal processes [15]. Although some heavy metals, at certain concentrations, are essential for the correct functioning of metabolic processes in human beings [16], the bioaccumulation of these components and repeated long-term exposure can result in toxic, neurotoxic, carcinogenic, mutagenic or teratogenic effects [3]. They also represent serious threats to the fauna and flora of the receiving water bodies.

Nickel (Ni) is a transition metal that occupies the 5th place as the most abundant element on earth, that is, 3% of its total composition [17]. Also, it is recognized as one of the most dangerous heavy metals due to its health related effects [18]. A typical effect of exposure to nickel in humans is dermatitis, but severe poisoning causes headache, dizziness, nausea and vomiting, chest pain, tightness of the chest, dry cough and shortness of breath, rapid respiration, cyanosis and extreme weakness. Excessive intake of nickel cause cancer of lungs, nose and bone [19]. Nickel, at low concentrations, is an essential heavy metal for several living beings. In the human body, for example, it allows to produce blood cells. In modern technologies, nickel is widely and increasingly used because its convenient physical and chemical properties [17]. Different industries produce a significant content of nickel, among other heavy metals, in industrial wastewater streams. For example, the process of electroplating, petroleum refining, printed circuit board (PCB) manufacturing and mining operations produce industrial waste water streams with alarming contents of nickel inorganic pollutant [20]. Thus, due to its extensive use, it can enter to human's biological system through different via and progressively accumulate at concentrations that exceed the suggested limits by international authorities. As water is essential for almost all life forms, it is important to preserve its quality avoiding the presence of agents that threatens life and life quality.

2.1.4 Drinking water standards

Considering the increasing problems related to public health, the World Health Organization (WHO) was set up on April 7, 1948. Nowadays, this date is celebrated every year as World Health Day. This organization is an international authority on public health and water quality, one of its main commitments is to give a healthier future to people all over the world ensuring the air, food, water, medicines and vaccines safety. To achieve this goal, they promote health-based regulations to governments. Regarding water safety, WHO produces international norms on water quality as guidelines. These guidelines for drinking water quality (GDWQ) are used in turn as a base for regulation and standard-setting worldwide. A lot of countries around the world implements its recommendations according to its context and health-based targets. [21]

In Ecuador, the Instituto Nacional de Normalización (INEN) is the national authority for standardization and technical regulation of quality of products and services. This institution set a technical standard named NTE INEN 1108 which is an adaptation of the GDWG of WHO, 4th. Ed, 2011. This standard establishes the requirements that drinking water must meet for human consumption (within the scope of scientific and technological knowledge) and applies to drinking water of public and private supply systems [21]. Drinking water supply systems must meet certain physical characteristics in addition to the allowed maximum limits of microorganisms, inorganic, organic and radioactive substances. Also, drinking water supply systems must comply with the regulation of good manufacturing (production) practices of the Ministry of Public Health. Regarding to the presence of heavy metals (inorganic materials), more specifically nickel, the NTE INEN 1108 standard allows 0.07 mg/l [22]. As the Constitution of the Ecuadorian Republic, in article 52, establishes that people have the right to dispose of goods and services of optimum quality, the violation of these rights entails law penalties [23].

2.1.5 Heavy metals removal

Researchers around the world are constantly developing methods to remove or at least reduce heavy metals levels in water sources of human consumption. This is due to the decreasing drinking water resources, rising sewage disposal costs, and more stringent discharge regulations that have limited acceptable levels of pollutants in water [15]. Three key general factors have to be taken into account when choosing the

most suitable method for heavy metals removal: the technical applicability, plant simplicity and cost-effectiveness [24]. There are a lot of methods (physicochemical and biological) that can be applied in order to remove or reduce heavy metals from water [25]. Although biological methods present a higher percentage of heavy metals removal, a low cost and are environmentally friendly, they need large areas and proper maintenance operation and among other characteristics which, in the end, makes it a highly expensive method [25]. In the case of physicochemical methods, its advantages and disadvantages are somehow balanced. On the one hand, physicochemical methods show in most cases a rapid process, ease of operation and control, it allows various input loads, does not require a large space and have a low installation cost. But on the other hand it shows expensive operational costs due to the use of chemicals, high-energy consumption and handling costs for toxic residues disposal. If last disadvantages could be improved, then physicochemical treatments are most suitable treatments for heavy metals removal [24]. The most used physicochemical methods are chemical precipitation, membrane filtration, electrodialysis, ion exchange and adsorption with new adsorbents [20]. Their advantages and disadvantages in application are presented in the next table:

Table 1. Advantages and disadvantages of physicochemical methods in application.

Treatment method	Advantages	Disadvantages	References
Chemical Precipitation	Low capital cost, simple operation	Residues generation, the extra operational cost for residues disposal	[24]
Adsorption with new adsorbents	Low cost, easy operations conditions, very low concentrations, high metal binding capacities	Low selectivity, production of waste products	[5]
Membrane filtration	Small space requirement, low pressure, high separation selectivity	High operational cost due to membrane fouling	[24]
Electrodyalisis	High separation selectivity	High operational cost due to membrane fouling and energy consumption	[26]
Ion exchange	Removal of metal and organic pollutant simultaneously, less harmful by products	Long duration time, limited applications	[27]

Note: Table taken from the book "Modern Age Waste Water Problems: Solutions Using Applied Nanotechnology".

Even when the diverse methods for water treatment offers great advantages (**Table 1**) and high removal efficiency [24], no individual treatment is universally effective and applicable for heavy metal removal[2]. During the last few years several studies on adsorption and ion exchange for water treatment had been developed. These methods have turn out to be the preferred one's techniques for removal of toxic contaminants from water because they are applicable at very low concentrations, due to the existence of low-cost adsorbents, occasional capital investment and ease of operation. Also, the sludge generation is not highly significant and offering the opportunity of regeneration and reuse [28].

2.2   ASORPTION AND ION EXCHANGE

Heavy metal cations can be immobilized to be removed in different materials, mainly by adsorption and ion exchange processes.

2.2.1 Adsorption

Adsorption is a physicochemical process consisting of an accumulation or concentration on a surface or interface of substances[29]. The substance adsorbed is identified as adsorbate and the substance on which adsorption takes place is known as adsorbent. The process generally is developed within a framework of oil-liquid, gas-liquid, gas- solid and liquid-solid[29]. The adsorbate in the latter case is the material that concentrates on the solid or adsorbent phase surface. Solids that have a high surface are used as adsorbents[30]. There are three types of forces with which the adsorbate is retained in the adsorbent, these are: electrical, van der Waals, and chemical. Depending on these forces (or interaction), adsorption can be classified into two groups: chemisorption and physisorption[31]. Chemisorption occurs when there is a chemical interaction between the adsorbate and the adsorbent, the adsorbed molecules are not allowed to move freely on the surface or within the interface. Physisorption, on the other hand, occurs when the adsorbed molecule is not fixed at a specific place on the surface, and it moves freely within or on the interface. In the cases in which the adsorption process is dominated by electric and Van der Waals forces, physical adsorption predominates[31].

2.2.2 Ion exchange

Ionic exchange process occurs when there is a substitution of an ion by another of the same charge that is fixed to an insoluble solid called exchanger. In the study of ion exchange, equilibrium between the solution and the adsorbent solid is assumed at all times, for which the exchange process is described with the following reaction:

$$A^+ + B\text{-}R \rightleftharpoons B^+ + A\text{-}R$$
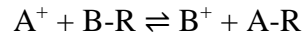
where A^+ and B^+ are the exchange cations, and R represents the mineral exchanger. [32]

2.3 ADSORBENTS

Adsorbent materials are used to clean or treat contaminated water through different mechanisms. These adsorbents can be natural organic, natural inorganic, or synthetic materials. In particular, natural adsorbents are preferred because they offer sustainable and cost-effective solutions for the remediation of polluted water.

2.3.1 Clays

Clays is the general term used to refer to materials that are present in nature, composed primarily by minerals fine grained that shows a plastic or hard behavior depending on its water contents. It is defined as a fine grained because there is no specific particle size accepted by the different branches of science, for example, colloid science use a particle size of 1 µm for clays but in geology the particle size used for clays is <2 µm [33].

Clays structure

Clays minerals are one of the phyllosilicates, or sheet silicates, subgroups. Phyllosilicates are regular crystals whose basic unit is the tetrahedron. The tetrahedron is constituted of a central silicon atom and four oxygen atoms at the corners $(SiO_4)^{-4}$ (Figure 1). When six tetrahedron join, form a ring. Interconnected rings share three of the four oxygen atoms of one tetrahedron, rendering a basic unit structure $Si_2O_5^{2-}$ (Figure 2, left). Most of the rings contain a hydroxyl ion in its center, then the basic unit structure becomes $Si_2O_5(OH)^{3-}$. (Figure 2, right). Interconnected six-member rings outspread in infinite sheet, tetrahedral sheet (type T).
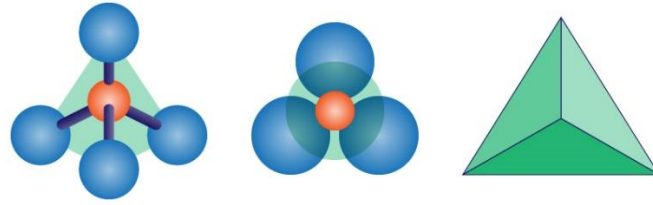
Figure 1. Si-O bonds within this tetrahedral structure. Taken from webpage Vision learning, Rock and Minerals, The silicate mineral [34].
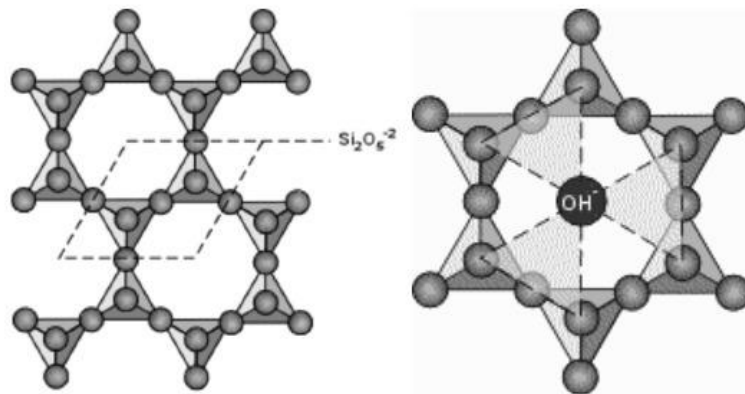
Figure 2. Six silicon tetrahedron interconnected to form rings (Left). Rings containing hydroxyl groups in its centre (Right). Taken from Phyllosilicates (Sheet Silicates) by Nelson, 2015

There are other polygonal bodies that can be joined together to form chains, as in the case of octahedral. Octahedron has a central cation, usually Fe^{+2}, Mg^{+2}, or Al^{+3}. These cations are present in octahedral coordination with the O^{-2} and OH^- ions of the tetrahedral layer (T), forming octahedral sheets (Type O) (Figure 3). Surface triangles formed by tetrahedral sheet become the faces of the octahedral groups.

Figure 3. Octahedral sheet structure.[35]

Clay classification

There are two groups of clays, T-O (1:1 sheet) and T-O-T (2:1 sheet). The union of a T-type sheet and an O-type sheet gives rise to the group 1 or T-O sheet. The union of two T-type and an O-type sheet (in the center) gives rise to group 2 or T-O-T sheet, also known as sandwich structure (Figure 4). The last one is the most complete and does not accept a new addition due to saturation of bonds [36,37].
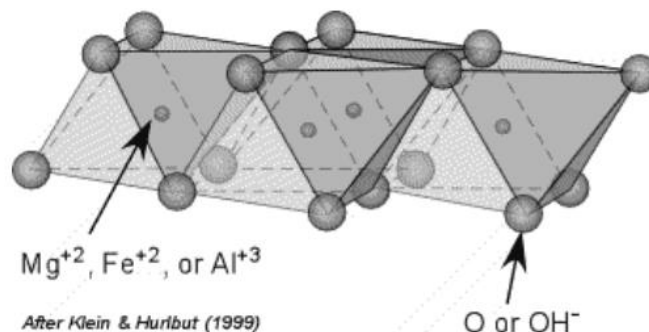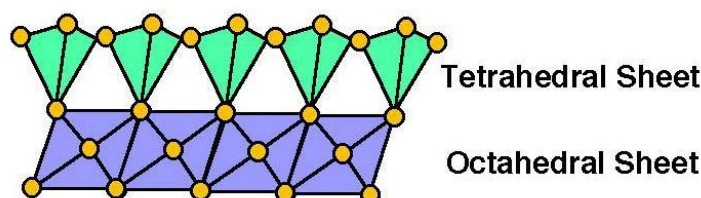

Figure 4. "T-O-T" sheet stacking pattern. [38]

Montmorillonite

Montmorillonite is a smectite, a subdivision of clays from group 2. The name derives from a clay mineral discovered in 1874 by Damour and Salvetat in the town of Montmorillón Vienne, France [39]. It is a T-O-T sheet composed of silicate tetrahedral layer and alumina octahedral layer joined by van der Waals forces. The isomorphic substitution of Al^{+3} by Mg^{2+} in the octahedral layer, and/or Si^{4+} by Al^{3+} in the tetrahedral layer produces a charge decompensation in the T-O-T sheet. The negative charge generated is neutralized with alkaline and alkaline earth cations (Na^+, Li^+, K^+, Ca^{2+}), and water molecules between the layers; which can be exchanged for other cations and/or molecules. At the edges of the clay, additional negative charge develops, which is generated when the structure is interrupted, and by broken bonds. They carry a variable charge that depends on the pH, which causes the protonation and deprotonation of the hydroxyl groups on the surface [40]. The chemical formula of montmorillonite clay is:

$$Na_{0.2}Ca_{0.1}Al_2Si_4O_{10}(OH)_2(H_2O)_{10}$$

Montmorillonite has physicochemical properties such as plasticity, particle size around 1μm, high specific surface (700 - 800 m^2), hydration and swelling capacities

of the interlaminar surface, and high cation exchange capacity (80-100 meq / 100g)[36,41]. In the ion exchange it has been shown that 80% occurs in the interlaminar space, and 20% is due to the charges on the edge of the sheets. [41]. Due to these properties several studies have been carried out in relation to the use of clays for removal inorganic contaminants[42]. The adsorption of heavy metals on montmorillonite is demonstrated by infrared spectroscopy analysis, X-ray diffraction, SEM, EDS, among others; performed to explore the interactions between inorganic compounds, soil cations, and water in the interlaminar clay space [37]. A high number of works have been reported in which the modifications of natural clays were done to carry out the adsorption of metals from aqueous solutions [43]. Acid activation of montmorillonite has been found to enhance adsorption of Ni(II) [28]. Montmorillonite (2 g/L) take up Ni(II) to the extent of 17.3 mg g^{-1} [18].

2.3.2 Diatomaceous earth

Diatomaceous earth, also called diatomite, are fossilized skeletons of microscopic unicellular aquatic plants (most common types of phytoplankton) called diatoms. The name diatom means "cut in half" in Greek, this is because diatoms cell walls (frustules) usually consist of two sides with an evident split between them. These microscopic organisms extract silica ($SiO_2.nH_2O$) from water bodies to render a microporous skeleton. When microorganism's life cycle ends, the organic matter decomposes and skeleton remaining is accumulated as inorganic sedimentary deposits. As these sedimentary deposits are abundant in the earth crust, diatomite is easily available at a low cost [6,44–46].

Structure, properties and applications

The structure of the diatomite is complex and varies in shape and architecture among species from which they are derived (Figure 5). The characteristic chemical composition of oven-dried diatomaceous earth is 80–90% silica, with 2–4% alumina (attributed mostly to clay minerals) and 0.5–2% iron oxide. In general, it contains numerous microscopic fine pores (as small as 0.1 microns), cavities and channels and therefore its physical and chemical characteristics are such as a high surface area, high adsorption capacity and low density. These characteristics makes diatomite a very useful material with a wide range of applications, such as in filtration and as

adsorption. Then, diatomite is able to take up particles from fluids at water treatment procedures [44].
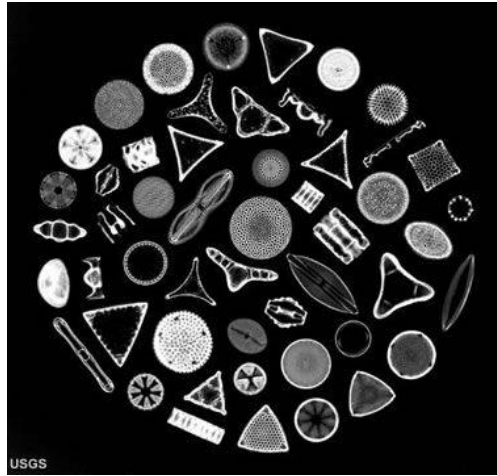
Figure 5. Frustules of fifty different diatom species. Photograph by Randolph Femmer, is public domain from USGS Library of Images from Life.

Diatomite surface contains silanol groups that spread over the matrix of the silica (Figure 6). The silanol can react with many polar organic compounds by various functional groups [47]. The surface properties of the diatomite such as hydrophilic in nature, acidity, ion exchange and adsorption capacities, are controlled by the presence of water, which is partially and structurally connected to the network of crystals of the diatomite, forming active hydroxyl groups on them [48].

Figure 6. Structure of silica surface depicting the various types of bonds and silanol groups present.[49]

2.3.3 Chitosan

Chitin is a mucopolysaccharide found widely in nature, it shows physical characteristics such as hardness, inelasticity and white color. It is a nitrogenous compound that can be obtained from different sources, but mainly in shells of marine species of crustaceans such as shrimp, crab and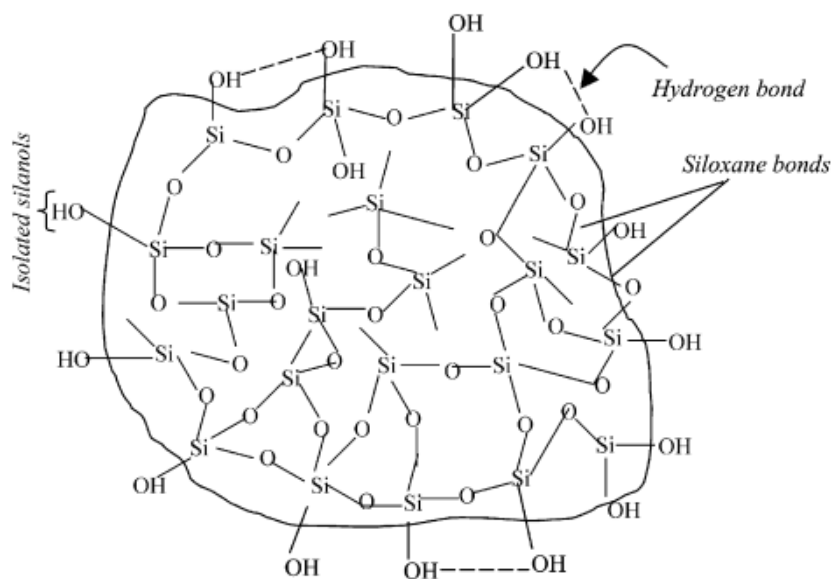 lobster. Chitosan is commercially produced from chitin by its deacetylation or removal of acetyl groups by alkaline treatment. [50]. After the process of deacetylation and drying, chitosan flakes are produced. These flakes can be milled until obtain fine mesh chitosan.

Structure, Properties and applications

Chitosan is a polysaccharide consisting of of randomly distributed β-(1→4)-linked D-glucosamine (deacetylated unit) and N-acetyl-D-glucosamine (acetylated unit) (Figure 7). The high activity of chitosan is due to two reasons, the first one is the presence of primary and secondary hydroxyl groups on each repeat unit, and second one is the presence of the amine group on each deacetylated unit. It shows special properties such as hydrophilicity, biocompatibility, biodegradability, non-toxicity, adsorption properties, etc. [51]. These properties make chitosan very useful material for different applications. Regarding to adsorption, chitosan can be used to remove heavy metals due to the presence of mentioned functional groups, which can serve as the

active sites. The mechanical and physical properties of chitosan can be altered by chemical modification of reactive groups present.
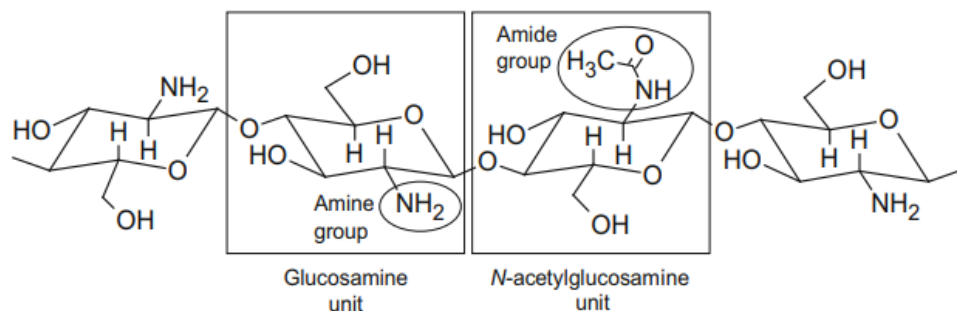
Figure 7. Structures of chitin and chitosan. Chitin (>40% amide groups); Chitosan (60% amine groups).

Currently, several studies about removal of metal ions using chitosan have been done in order to found the sites in which a divalent metal can be linked to the structure of the chitosan. Three principal ways in which the interaction can occur have been found (Figure 8). One way is when the metal forms bonds with two different amino groups, other is when the metal forms a bond with an amino group of one of the chains of the structure and another bond with an oxygen from another chitosan chain, and finally the third way is the case in which the metal forms two bonds with oxygen in different chains [52].

Figure 8. Possible chelation mechanisms of chitosan.

2.4 ADSORPTION ISOTHERMS

Adsorption isotherm is a curve that expresses the variation in the amount of gas adsorbed by the adsorbent with pressure at constant temperature [53]. These isotherms describe the dynamic process of adsorption through fitting mathematical models to experimental data. The most commonly used models that describe the solid-liquid adsorption process are:
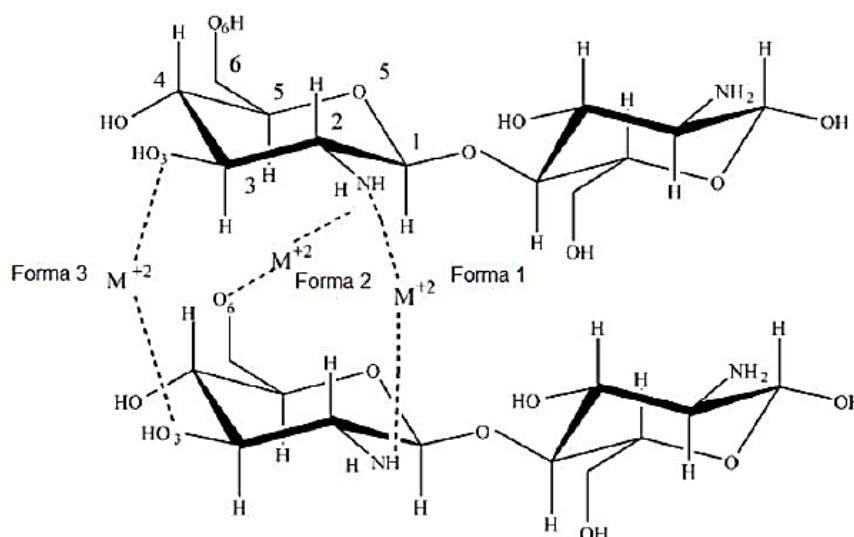
a) Langmuir isotherm

A monolayer sorption is described Langmuir isotherm. It is determined that the adsorbent contains a finite number of identical binding sites (homogenous surface). The linear form of the Langmuir equation [54] is expressed in **Table 2**.

b) Freundlich isotherm

A multilayer adsorption is described by Frerundlich isotherm. A heterogeneous surface of the adsorbent is determined for adsorbents that fits this model. The linear form of the Freundlich equation [53] is expressed in **Table 2**.

Table 2. Langmuir and Freundlich equations and parameters.

Model	Equation	Parameters
Langmuir	$\dfrac{Ce}{Qe} = \dfrac{1}{Q_m \cdot K_L} + \dfrac{Ce}{Q_m}$	Qe is the amount of Ni^{2+} per unit mass of adsorbent (mg/g) K_L is the Langmuir constant related to the adsorption capacity (L/g) Ce is the concentration of adsorbate in the solution at equilibrium (mg/L) Q_m is the maximum uptake per unit mass of carbon (mg/g)
Freundlich	$ln(Qe) = ln(K_F) + \dfrac{1}{n} ln(Ce)$	Ce and have the same meaning as in the Langmuir isotherm K_F is the Freundlich constant n is the empirical parameter representing the energetic heterogeneity of the adsorption sites (dimensionless)

2.5 CHARACTERIZATION TECHNIQUES

2.5.1 X ray Diffraction

X-Ray Diffraction (XRD) is a nondestructive analytical technique, through which crystalline solids can be characterized. Important information about structure, phases, preferred crystal orientations (texture), crystallinity and other structural

parameters can be obtained. Constructive interference of a monochromatic beam of X-rays scattered at specific angles from each set of lattice planes in a sample produce X-ray diffraction peaks. This constructive interference is only possible when conditions satisfy Bragg's law. This law relates the radiation wavelength (λ) to the distance between the planes with hkl (d_{hkl}) indices and the incidence angle (θ_{hkl}), by the following equations:

$$n\lambda = 2dsin(\theta_{hkl})$$

The distribution of atoms within the lattice determine the intensities of the peaks. Therefore, the X-ray diffraction pattern is the fingerprint of periodic atomic arrangements in a given material. [55]

Clays studies by XRD are based on their interplanar distance $d_{(001)}$, which varies depending on the compensation cations present and on the state of hydration, these changes are reflected in the direction of the axis. The expansion of clay structure, also, takes place with the access of organic compounds into the interlaminar space. In natural deposits, montmorillonite forms a monoclinic crystal (C2/m group), which usually possess some potassium and iron impurities. [36,56]. Diatomaceous earth may show a certain degree of crystallinity while chitosan, as it is an organic compound, do not present crystallinity.

2.5.2 Infrared spectroscopy

Infrared spectroscopy (IR) utilizes the fact that molecules absorb specific frequencies of light that are characteristic of their structure. These absorptions occur at resonant frequencies, that is, the frequency of the absorbed radiation corresponds to the vibrational frequency. The energies are dependent on the shape of the molecular surfaces, the associated vibration coupling, and the mass corresponding to the atoms. IR equipment radiates a monochromatic light beam at a sample and measure how much light a sample absorbs at each wavelength. [57]

For minerals, the spectrum provided by IR spectroscopy gives valuable information such as mineral structure, the family of minerals to which the specimen belongs, the nature of isomorphic substituents and the existence of crystalline and noncrystalline impurities. Montmorillonite clay and diatomaceous earth characteristic

vibrations are due to hydroxyl groups and the silicon–oxygen network [58]. In the case of chitosan, amide I and II vibrations are characteristic.

2.5.3 Energy-Dispersive Spectroscopy

The electron beam interaction with a chemical sample produce a range of emissions, one of these emissions are X-rays. An energy-dispersive (EDS) detector is used to distinguish the characteristic X-rays of the various elements present in the sample into an energy spectrum, and EDS device software is used to analyze the energy spectrum in order to determine the abundance of specific elements. EDS can be used to find the chemical composition of materials up to a spot size of a few microns, and to create maps of the composition of elements across a much wider raster area. [59]

2.5.4 Scanning Electron Microscopy

Scanning electron microscope (SEM) is a type of electron microscope which produces sample images by scanning the surface with a focused electron beam. The electrons interact with atoms in the sample, producing various signals containing information about the topography of the surface and the sample composition. In a raster scan pattern, the electron beam is scanned, and the beam's position is combined with the intensity of the detected signal to produce an image. In the most common SEM mode, a secondary electron detector (Everhart-Thornley detector) is used to detect secondary electrons released by atoms that are excited by the electron beam. Among other things, the number of secondary electrons that can be detected, and hence the signal intensity, depends on specimen topography. A resolution better than 1 nm can be achieved. [60]

2.5.5 Ultraviolet-visible Spectroscopy

Ultraviolet-visible spectroscopy (UV-Vis Spectroscopy) makes use of absorption spectroscopy in ultraviolet and visible wavelength ranges—180–380 nm and 380–750 nm, respectively—for characterizing molecules[61]. It is used to determine, among other things, the concentration of a solution. The radiation energy that passes through a sample in ultraviolet and visible wavelength decreases in relation to the distance it travels through the absorbent medium, and decreases with the concentration of ions or absorbent molecules present in the medium. These two factors determine the proportion of the total incident energy that is transmitted. The decrease in

monochromatic radiation energy that passes through a homogeneous absorbent medium is quantitatively established by the Beer-Lambert law which stablishes that the absorbance of a solution is directly proportional to the concentration of the solution. The UV/Vis spectrophotometer measures the intensity of light (I), which passes through a sample, and compare it to the intensity of light before passing through the sample (Io). The transmittance (% T) is obtained from the I / Io ratio:

$$Absorbance \ (A) = -(\%T)$$

This absorbance is a function of the wavelength of the incident radiation, so that the spectrum that relates these two variables is characteristic for each compound. In the case of Ni^{2+}, it absorbs at a characteristic wavelength of 430 nm [62].

2.5.6 Brunner-Emmett-Teller surface analysis

The BET theory (abbreviated from Brunner-Emmett-Teller theory) is a powerful technique used for the calculation of solid or porous material's surface area and pore size through gas adsorption[63,64]. Surface area of a material provides important data about how solid interacts with its environment. Some properties such as rate of dissolution, catalytic activity, moisture retention and shelf life are also associated to the surface area of a material[65].

This theory allows estimating the surface area of the solid media from the monolayer capacity and knowledge of the cross-sectional area of the probe molecule (nitrogen: 16.2 $Å^2$/ molecule)[63]. Generally, it involves exposing the solid under investigation to nitrogen (probe molecule) at liquid conditions (i.e. 77K). The relation between the physiosorbed nitrogen molecules in the solid and the constant pressure of the gas at constant temperature can be represented in adsorption isotherms. The isotherms obtained correspond to the process of adsorption and desorption of gas in the solid, when the adsorption isotherm does not coincide with that of desorption, a hysteresis appears[65,66]. Isotherms can be classified into six types[64] as shown in Figure 9:
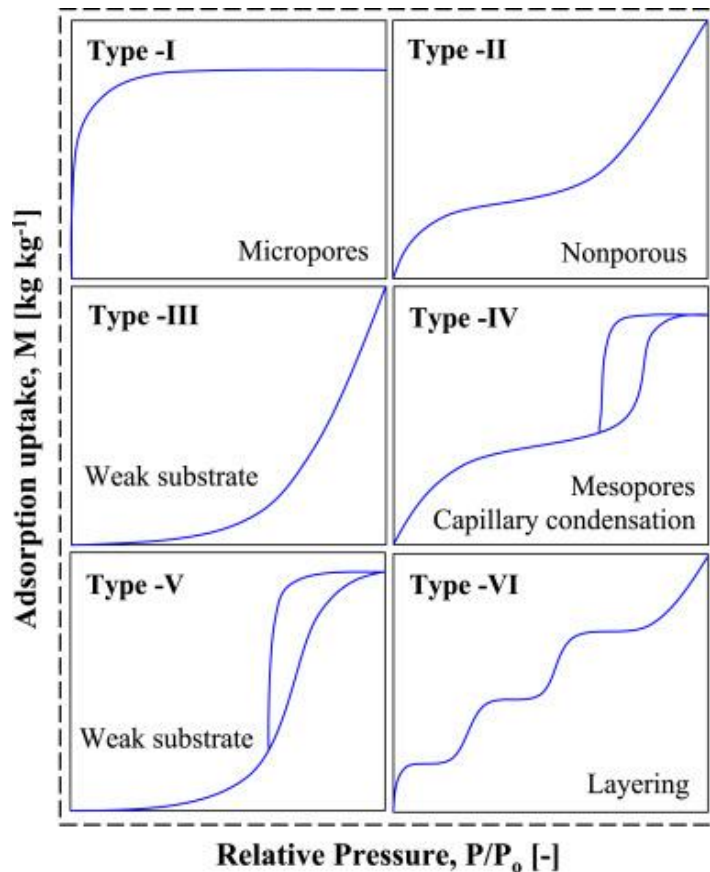
Figure 9. Classification of adsorption isotherms[67]

Type I isotherms can be described by the Langmuir equation[66]. Chemical adsorption often produces this type of isotherm where the asymptotic approach to a limiting value of adsorbed mass indicates that the surface sites are completely occupied[65]. In the case of physical adsorption, type I isotherm is characteristic for microporous materials with small external surface showing micropore filling but no multilayer adsorption[65,66].

Type II isotherms describe frequently adsorption in nonporous solids or in microporous materials (pore diameter > 50nm)[64,66]. The inflection point of the isotherm indicates the completion of the first adsorbed monolayer and the beginning of multilayer adsorption[65].

Type III isotherms occur in systems where the adsorbate- adsorbate interaction is greater than the interaction between adsorbate-sorbent[66].

Type IV isotherms are frequently observed in special mesoporous materials. It is characterized by a hysteresis curve caused by pore condensation[66].

Type V isotherms are related to type III isotherm with weak adsorbate-sorbent interactions, but indicates the existence of mesopores in the solid[64].

Type VI isotherms represent stepwise multilayer adsorption[66].

For surface area determination BET isotherm is represented in its linearized form:

$$\frac{1}{V[(P_o/P) - 1]} = \frac{1}{V_m C} + \left(\frac{C - 1}{V_m C}\right)\frac{P}{P_o}$$

where V is the volume of adsorbed gas at partial pressure P of adsorbate, P_o is the nitrogen saturation pressure, V_m is the monolayer adsorbed gas quantity, and C is the BET constant.

The monolayer adsorbed gas quantity V_m and C can be determined with the values of the slope and intercept obtained by plotting $1/V[(P_o/P) - 1]$ against $/P_o$.

Then, surface area (S) can be derived with the following equation:

$$S = \frac{V_m A N}{M}$$

Where A is the Avogadro number, M is the molecular weight of adsorbate, and N is the adsorbate cross sectional area (0.162 nm^2 for nitrogen).

Chapter 3: Methodology

This chapter describes the design adopted by this research to achieve the aims and objectives stated in section 1.3 of Chapter 1. Section 3.1 discusses the materials and reagents used in the study, the sample preparation and adsorption studies implemented are shown in section 3.2 and section 3.3 respectively. Finally, section 3.4 lists all the instruments used in the study and justification of their use.

3.1 MATERIALS AND REAGENTS

The experiments were conducted with natural adsorbents: montmorillonite clay (M), diatomaceous earth (D) and chitosan (C). M and D were collected in the Northern Ecuador specifically in the town of Guayllabamba, while chitosan (deacetylation 87%, viscosity 1000 mPa.s, molecular weight ~190,000-310,000 g/mol) used was of analytical grade, procured from Aldrich Chemical Corporation (St. Louis, MO, USA). Every chemical reagent used were of analytical grade. Concentration and amounts of substances used are detailed in the following flow charts and also in text.

3.2 SAMPLES PREPARATION

3.2.1 Preparation of natural adsorbents

Clay tuff M and D were ground until a talcum powder was obtained. D was just washed with abundant deionized water and let dry overnight, while M clay had to undergo extraction and purification methods. Extraction process was carried out by pipette method (Figure 10) in order to separate fractions of other minerals such as sand and quartz. Purification methods were performed in order to remove carbonates (Figure 10B) and organic matter (Figure 10C), to allow a better dispersion of clay particles.
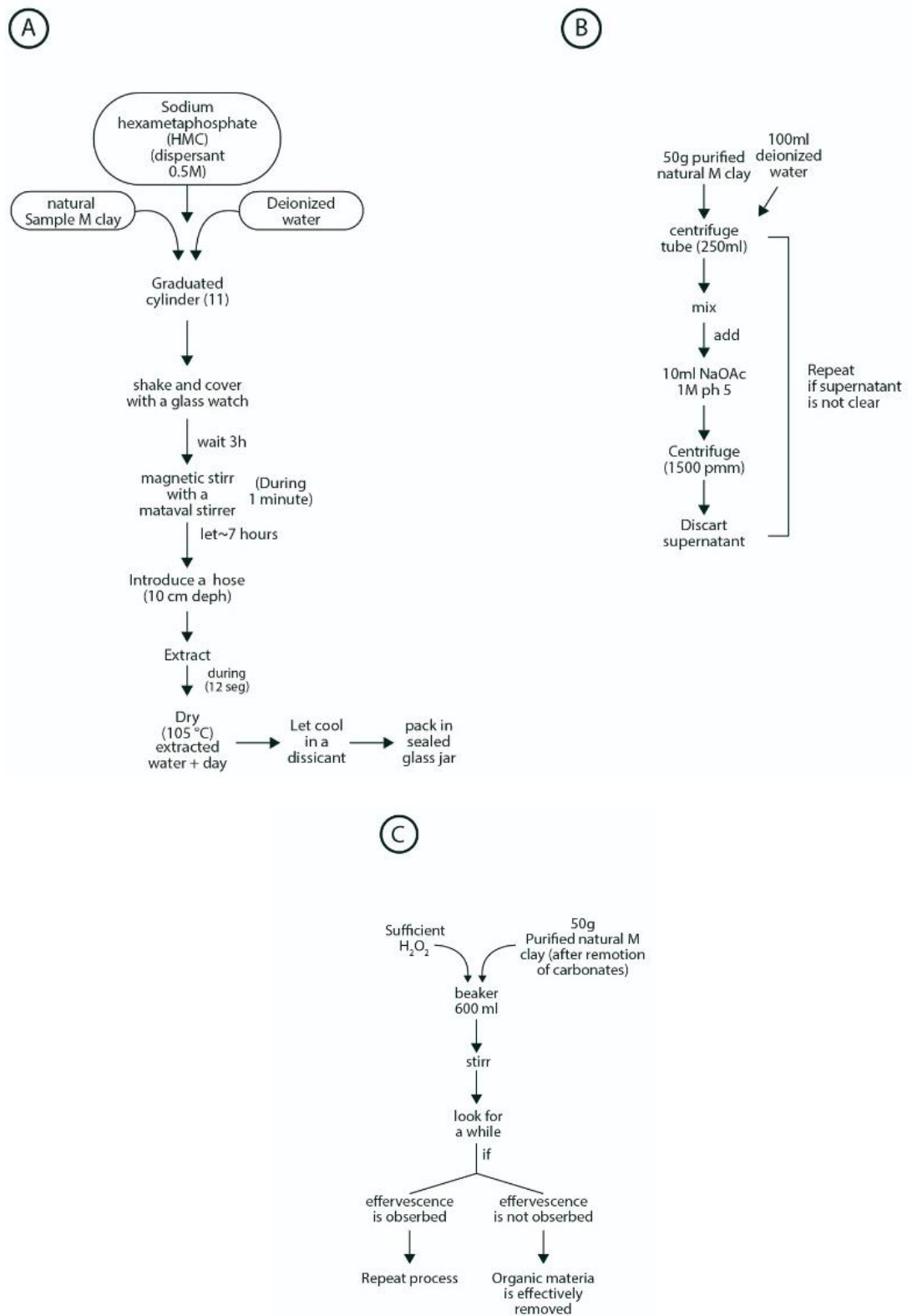
Figure 10. Flowcharts of pipette method (A). Removal of carbonates (B) and removal of organic matter (C)

Also an acid activation procedure (Figure 11) to montmorillonite clay was performed, in order to enhance its adsorption capacity, following protocol suggested in the literature [68]. The acid treatment of the montmorillonite was performed by contacting 40 g of natural montmorillonite with 200 mL of H_2SO_4 1.5 M in a 500 mL glass beaker. The mixture was stirred for 30 minutes and left for 24 h at room temperature conditions, then the aqueous phase was decanted. The clay residue was washed with abundant deionized water for several times and then sundried, after that, it was heated at 150 °C using an oven for 5 hours. The samples were then pulverized and passed through mesh sieves of sizes 100 to 500 μm.
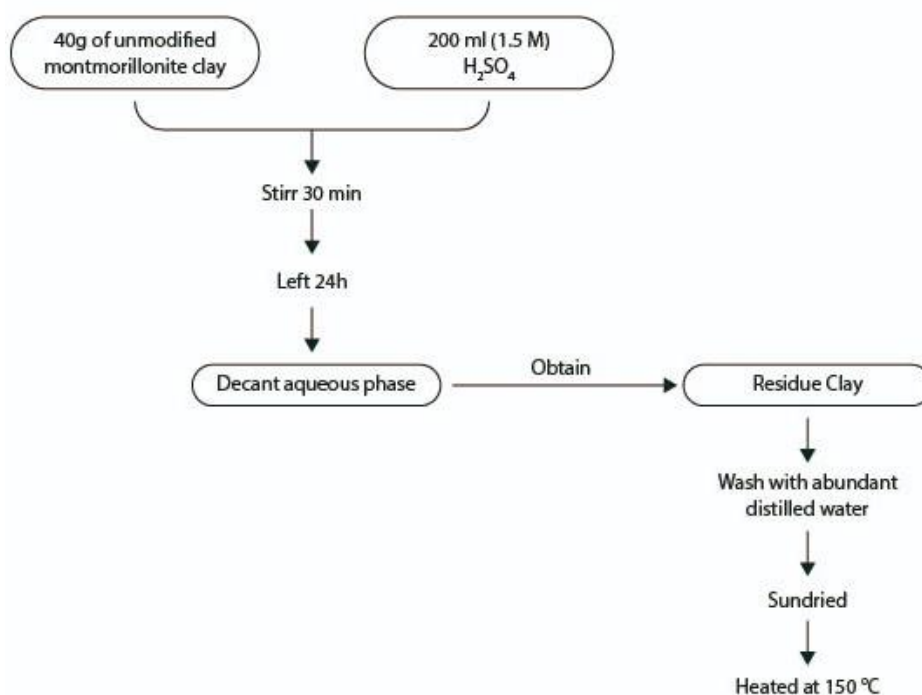

Figure 11. Schematic representation of Acid activation procedure.

3.2.2 Synthesis of composites

Composites were prepared by dispersion chitosan in montmorillonite (CM), in diatomaceous earth (CD) and both in a mixture of same proportion (CMD) (Figure 12). Their synthesis can be divided into two parts. In the first part, 2 g of chitosan were dissolved in 200 mL of 0.15 Mol/L oxalic acid solution under stirring and temperature conditions of 300 rpm at 60 °C. These conditions were maintained until viscous chitosan gel was obtained. Then, diatomaceous earth and/or montmorillonite

powder was slowly added into the chitosan gel (For CM: 4 g of activated natural montmorillonite clay; for CD: 4 g of natural diatomaceous earth and for CMD: 2 g of montmorillonite and 2 g of diatomaceous earth), keeping temperature and stirring conditions for three hours more to obtain a homogeneous mixture. In the second part, spherical beads of CM, CD and CMD were prepared by dropwise method. Using a syringe, the final gel mixture was dropped for each composite into 200 mL solution of NaOH (1M). Finally, the NaOH⁻ solution was decanted and the spherical composites were washed with deionized water for several times until neutralization, and then were dried in an oven at 70 °C for 12 hours. The prepared dried adsorbents were sealed in a vial. [6]
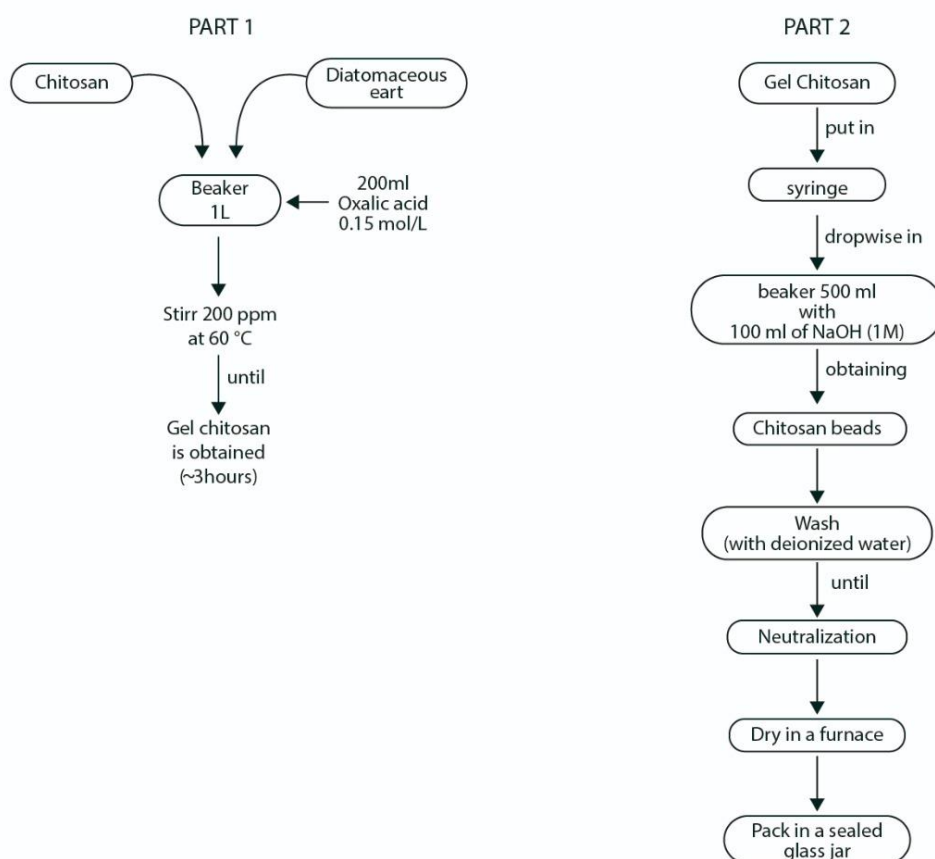

Figure 12. Schematic representation of the preparation of chitosan beads.

3.3   ADSORPTION STUDIES

3.3.1 Preparation of aqueous Ni^{2+} solutions

Stock solution (1062 ppm) of Ni^{2+} ions were prepared by acid digestion of solid nickel. The stock solution was then diluted to give standard solutions of concentration: 0.25, 05, 1, 2, 3 and 5 mg/L.

3.3.2 Adsorption equilibria experiments

Ni^{2+} adsorption from aqueous systems onto prepared adsorbents (M, D, CM, CD and CMD) were performed to determine their adsorption capacity at different conditions, to investigate mechanism of reaction involved (if any exist) as well as optimal experimental conditions. In a series of 50 mL plastic containers, 0.1 g of adsorbents was immersed in 25 mL each one of Ni^{2+} solutions (with initial Ni^{2+}concentrations of 0.25, 0.50, 1, 2, 3 and 5 mg/L) respectively, which were stirred (at 200 rpm). Different contact times were tested (1, 3 and 6 hours), for solution pH 2.0, 5.5 and 9.0 achieved by the addition of 0.1 M solutions of NaOH and HCl depending on the case. When contact time was completed, samples were taken out from the plastic containers, centrifuged (at 2000 rpm), filtrated and stored. In order to determine Ni^{2+} concentration after adsorption process, spectrophotometric analysis was performed.

Spectrophotometric analysis

To carry out absorbance measurements for Ni^{2+} solutions, this metal ion is first converted into a coloured complex using dimethylglyoxime 1% (DMG) which forms a red coloured complex (Ni-DMG) when treated with an alkaline solution of nickel in presence of an oxidising agent, in this case, water bromine.

Preparation of standards for the calibration curve: Six working standard Ni^{2+} solutions with different concentrations (0.25, 0.5, 1, 2, 3 and 5 mg/L) were prepared for calibration. Then, each Ni^{2+} solution was converted to a complex of Ni-DMG. Finally, the absorbance of each solution was measured by Uv-vis Spectrophotometer. The wavelength of maximum absorbance and absorbance values were recorded.

Calibration curve: The calibration curve was constructed by plotting the values of absorbance against concentration. According to the Lambert Beer law, it should be a straight line because they are directly proportional.

Determination of Ni²⁺ concentration after adsorption process: Each Ni^{2+} solutions after adsorption process was converted to a complex of Ni-DMG. Then aabsorbance measurements (at wavelength of maximum absorbance) of them carried out and recorded. From the equation given by calibration curve and recorded absorption values, Ni^{2+} concentrations after adsorption process were calculated.

The adsorption capacity, Qe (mg/g), was calculated using the following formula:

$$Qe = \frac{(Co - Ce)V}{W}$$

and the Ni^{2+} removal percentage *R*% was calculated as follows:

$$R\% = \frac{(C_o - C_e)}{C_o} \times 100 \%$$

Where Co is the initial concentration of Ni^{2+} solution, Ce is the concentration after adsorption process, V is the volume of the solution (L) and W the weight of adsorbent used (g).

3.4 CHARACTERIZATION EQUIPMENT

Naturals adsorbents and synthesized composites were analysed by the following characterization equipment:

X ray Diffraction

X ray-diffractometer with CuKα radiation (λ=1.5406Å) was used through X-ray powder diffraction technique with 0.02° step size, 0.42 step time and measurement range of 5-80 °. XRD patterns of the samples were obtained using a diffractometer Siemens D-500.

Infrared spectroscopy

FTIR spectrometer with KBr disc technique in the region of 400-4000 cm-1 was used in this research. FTIR spectra of the samples were recorded using a Nicolet model 205 spectrometer.

Scanning Electron Microscopy and Energy Dispersive Spectroscopy

Scanning electron micrographs and chemical composition were obtained using a Philips XL-30 scanning electron microscope equipped with a LINK-ISIS-EDS system.

UV-vis spectroscopy

All absorbance measurements were conducted on PerkinElmer Lamda 1050 UV-vis spectrophotometer using 1 cm matched glass cells in order to find Ni^{2+} concentrations in solution after adsorption process.

Brunner-Emmett-Teller surface analysis

BET model was used to determine surface area and pore volume estimation. N_2 isotherms and other textural properties were achieved using a sorptometer Micromeritics model 2010 at -196 °C.

Chapter 4: Results and discussion

In this chapter all the results of the study presenting interpretation, inference, and/or evaluation of them are detailed.

4.1 COMPOSITES CHARACTERIZATION

4.1.1 X-Ray Diffraction (XRD)

The XRD difractograms were obtained to confirm the nature and phases present in the clay sample and the composites prepared from it. To ensure the nature of clay, the diffractogram of natural activated montmorillonite was compared to a diffractogram reported in mineral database [69]. It is clear that both XRD patterns are very similar to each other as shown in the Figure 13, confirming that the used clay is a montmorillonite one.
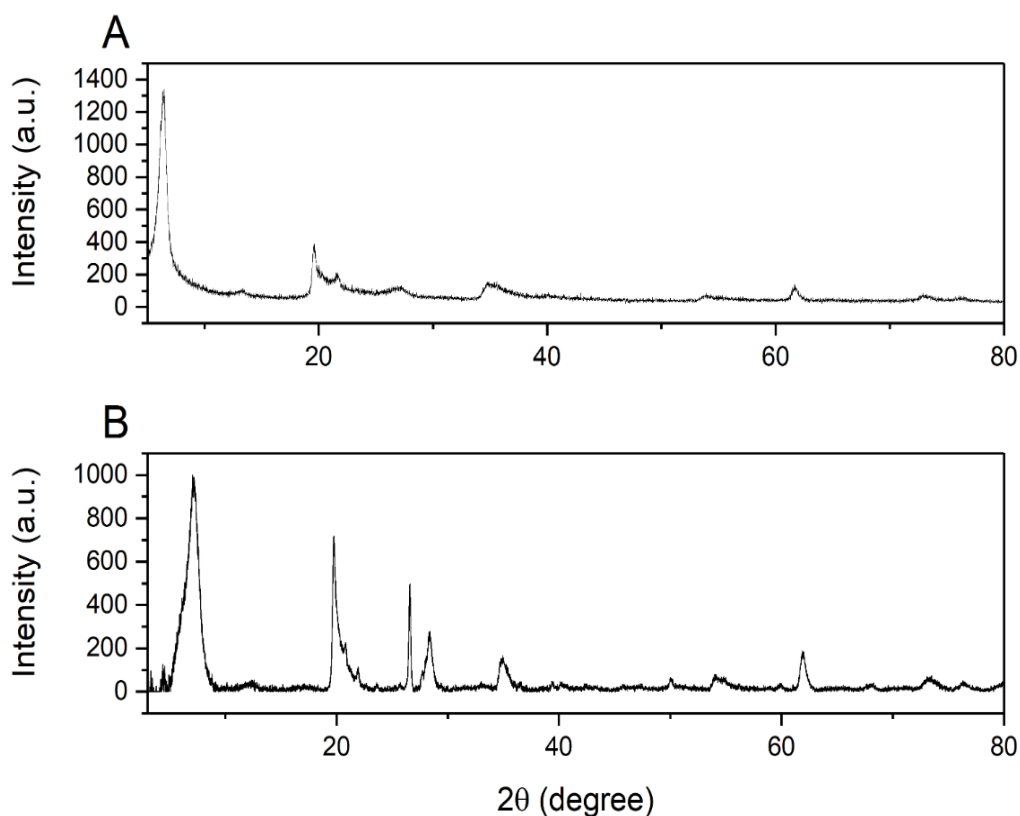

Figure 13. XRD diffractograms of montmorillonite clay A. Reported database and B. Experimentally obtained (obtained).

In is observed the XRD pattern for M. It shows the characteristic diffraction plane (001) at $2\theta = 7.049°$ with a corresponding basal spacing of 12.53 Å, normally, this plane would be localized at $2\theta \approx 6°$ with a d = 15 Å. However, the value can vary according the hydration of the montmorillonite and exchangeable cations. Other important diffraction plane observed in the XRD is (060) which indicates the dioctahedral structure of the clay [70], this diffraction plane is found in $2\theta = 61.97°$ as shown in the Figure 14. XRD difractogram for activated montmorillonite clay., with a basal spacing of 1.50Å. The other diffraction planes found in M difractogram illustrate the 2:1 clay which is classic for montmorillonite clay, confirming its nature, nevertheless, at 2θ between 26° and 28° are found signals corresponding to the α-quartz still present in the sample.
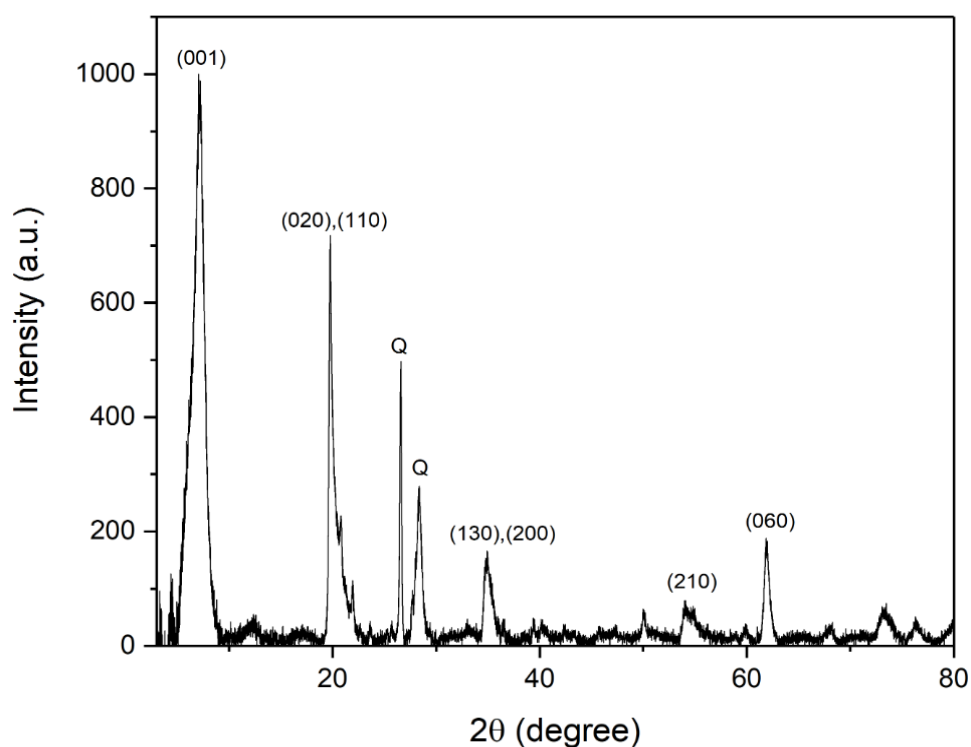

Figure 14. XRD difractogram for activated montmorillonite clay.

4.1.2 Fourier Transformed Infrared Spectroscopy (FTIR)

The FTIR spectroscopy was used to provide evidence of the presence of chitosan in composites, to ensure its coupling with montmorillonite clay (M) and diatomaceous earth (D).

The FTIR spectrum of commercial chitosan (Figure 15) shows characteristic peaks at 3360 cm^{-1} due to O-H stretching vibrations which can overlap the N-H stretching vibration. At 2919 and 2874 cm^{-1}, there are bands that confirms the presence of symmetric C-H stretcing in methylene group and C=O stretching in amides (Amide-I band) respectively. At 1640 cm^{-1} it is found a band for amide-II that may overlap with C-O stretch of acetyl group, the band at 1592 cm^{-1} belongs to the N-H bending in secondary amides (amide II band) that could be overlapping the C=C stretch of aromatic ring, bands between 1420–1377 cm^{-1} are attributed to asymmetric C-H stretching and bending of CH$_2$ group. [71]
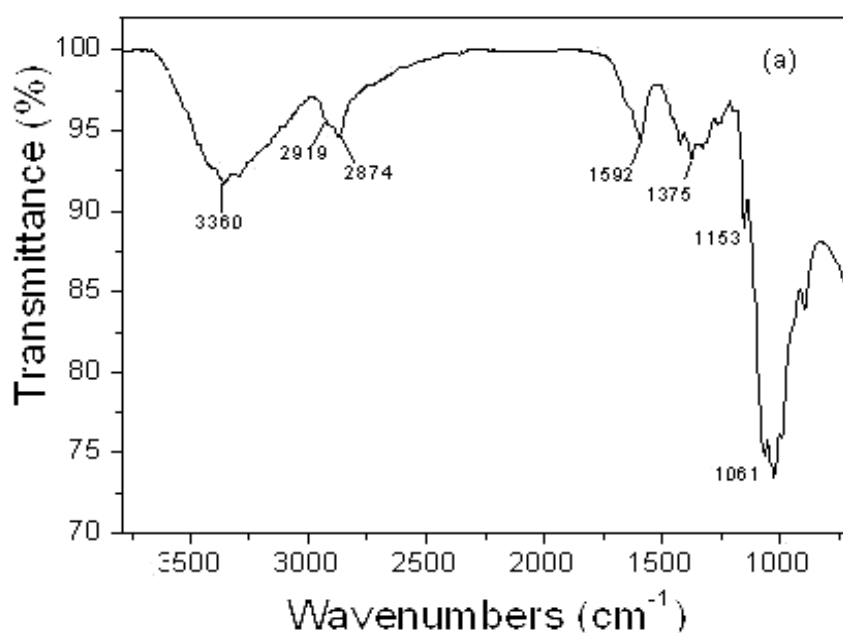

Figure 15. IR spectrum of commercial chitosan (Sigma-Aldrich).

For M clay (Figure 16), it is observed the presence of a band at 3628 cm^{-1} that arises from the stretching vibrations of O-H that corresponds to silanol (Si-OH) groups. Also, it is found a broad band near 3440 cm^{-1} attributed to O-H vibration of absorbed water in phyllosilicate. The band at 1641 cm^{-1} is due to H-O-H bending vibrations. Asymmetric stretching vibrations bands of Si-O-Si and Si-O-Al were found at 1119 and 1049 cm^{-1}, respectively. The peaks at 920 and 798 cm^{-1} corresponds to symmetric stretching vibrations of Si-O-Si and Si-O-Al, respectively. The bands at around 623, 528 and 467 cm^{-1} are due to the Si-O and Al-O bending vibrations (Al in octahedral coordination) [52,72]. For CM, it was found almost the same bands as M but,

in contrast, it is observed bands at 2920 cm^{-1} and 2824 that are attributed to C-H stretching vibrations, and bands in the range 1420–1377 cm^{-1} that can be due to the asymmetric C-H bending of CH_2. Each new band found is attributed to chitosan added to form the composite. There are other characteristic bands of chitosan that should be seen in the spectra but they could be overlapped with those of the phyllosilicate.
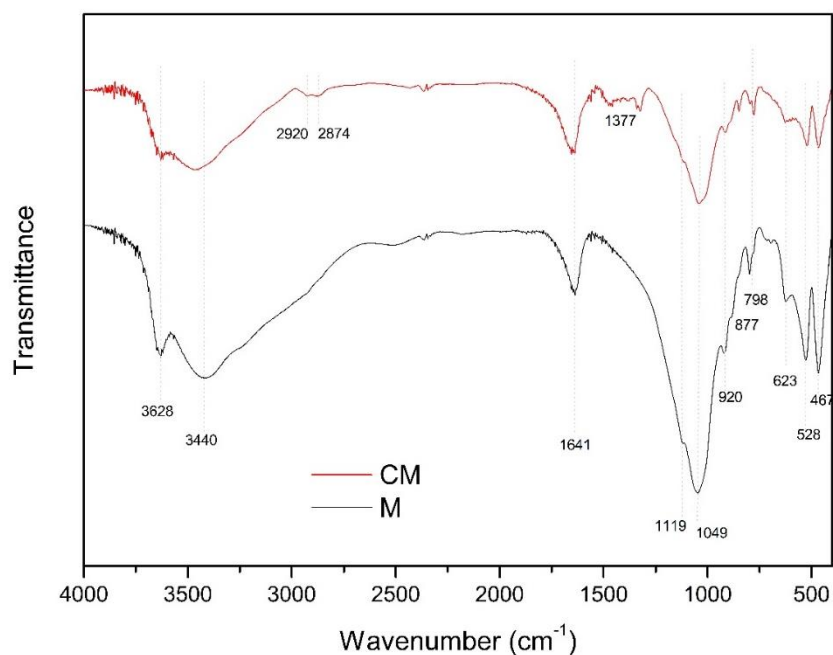

Figure 16. Comparison between FTIR analysis of montmorillonite clay (M) and the composite montmorillonite clay/chitosan (CM)

For D sample (Figure 17), it was found similar bands than those of M, which is expected because both materials are aluminosilicates. However, the D present less hydration degree and the bands due to the Al-O bending are not observed, possibly because of a lower amount of aluminum in the framework of diatomaceous earth. For CD, in addition to the bands found for D, extra bands were observed between 1450 and 1635 cm^{-1} which corresponds to C=N stretching, and at 2884 and 2924 cm^{-1} which are characteristic owing to C-H stretching vibrations. These extra bands are absent in the parental D which confirms the presence of chitosan in the composite. [73,74]
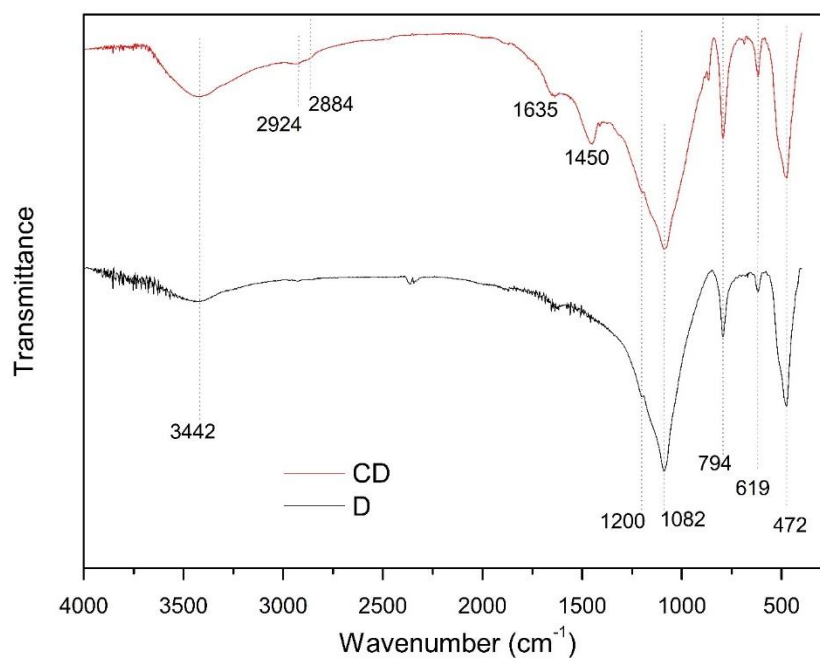
Figure 17. Comparison between FTIR analysis of diatomaceous earth (D) and the composite diatomaceous earth/chitosan (CD)

Figure 18 presents the FTIR of the composites prepared from chitosan-clay-diamite, in which it can be seen all characteristic bands of the different components, according to the previously discussed.
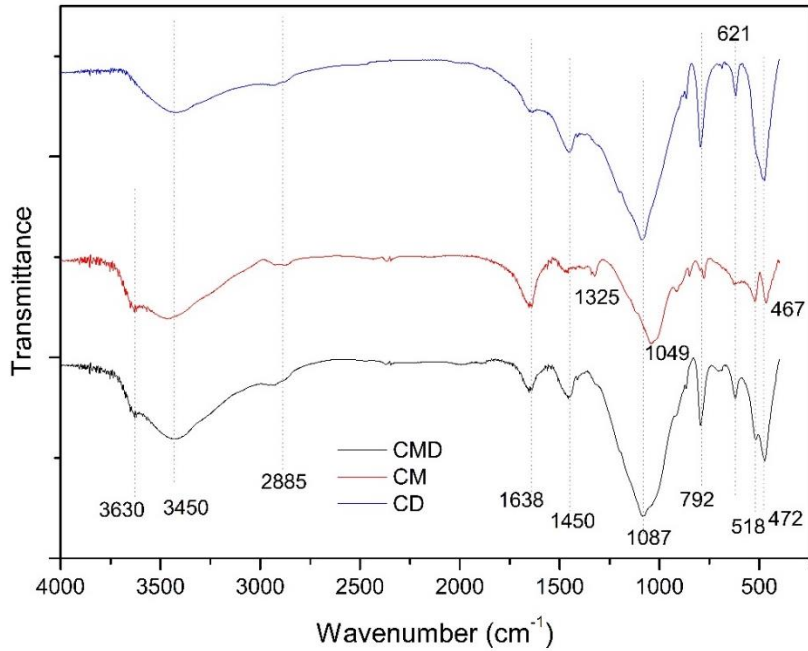
Figure 18. Comparison between FTIR analysis of composites.

4.1.3 Energy Dispersive x-ray Spectroscopy

The Energy Dispersive x-ray Spectroscopy (EDS) was used to confirm the elemental composition of montmorillonite clay, diatomaceous earth and synthesized composites.

For montmorillonite clay (Figure 19) it was found elements consistent with its chemical formula. The content of silicon is attributed to its presence in the tetrahedral layer of the clay, while aluminum content belongs to octahedral layer. Although, there can be some isomorphic substitutions of Si^{4+} by Al^{3+} in the tetrahedral layer. In a similar way, the presence of magnesium could indicate that occurs isomorphic substitution of Al^{+3} by Mg^{2+} in the octahedral layer. Both kinds of substitutions produce charges decompensation in the T-O-T sheets. The negative charges generated are neutralized with alkaline and alkaline earth cations which in this case are K^+ and Ca^{2+}. The presence of Fe^{2+} could be associated to impurities of iron minerals.

For diatomaceous earth, EDS elemental analysis showed (Figure 19) a typical composition of an silicate material with very low concentration of Al^{3+}. The presence of sodium could be related to Na^+ cations which are present as compensation cations. The elemental composition of diatomaceous earth based on the EDS analysis is consistent with its chemical composition.
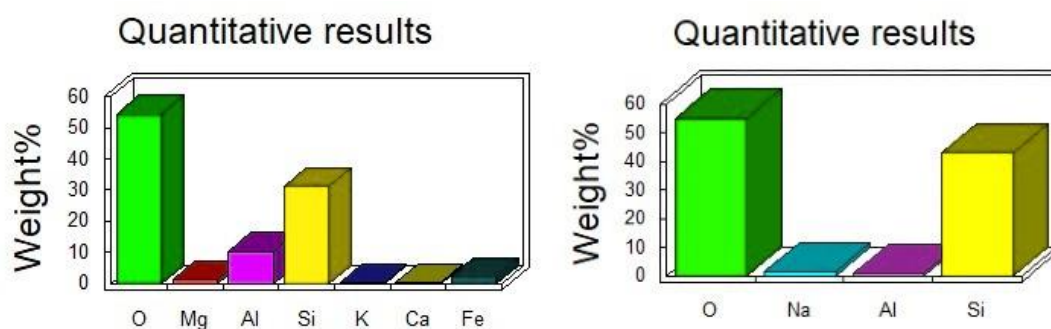
Figure 19. EDS for natural montmorillonite clay (left) and diatomaceous earth (right).

The EDS analysis of the composites CM, CD and CMD Figure 20 shows the presence of carbon and an increase in the oxygen content percentage which confirms the successful formation of the different composites.
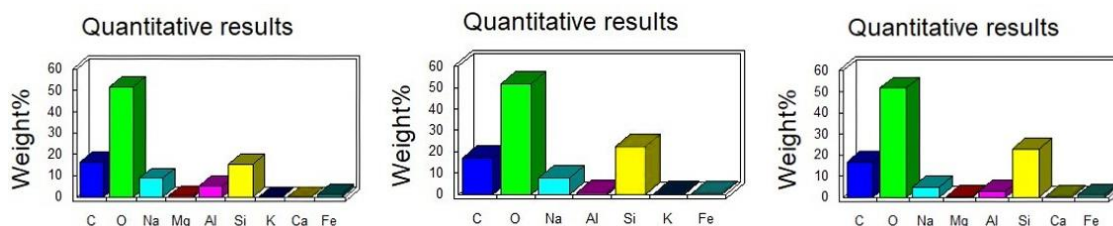
Figure 20. EDS for composites CM, CD and CMD from left to right respectively.

4.1.4 Scanning electron microscopy

In Figure 21**¡Error! No se encuentra el origen de la referencia.**, the SEM micrographies of natural activated montmorillonite clay (M) reveals that the surface morphology of M has a layered structure of different sizes which, according to literature, is characteristic of phyllosilicates[75]. Also, it presents a relatively rough heterogeneous surface.

Figure 21. SEM micrography of natural montmorillonite clay (M).
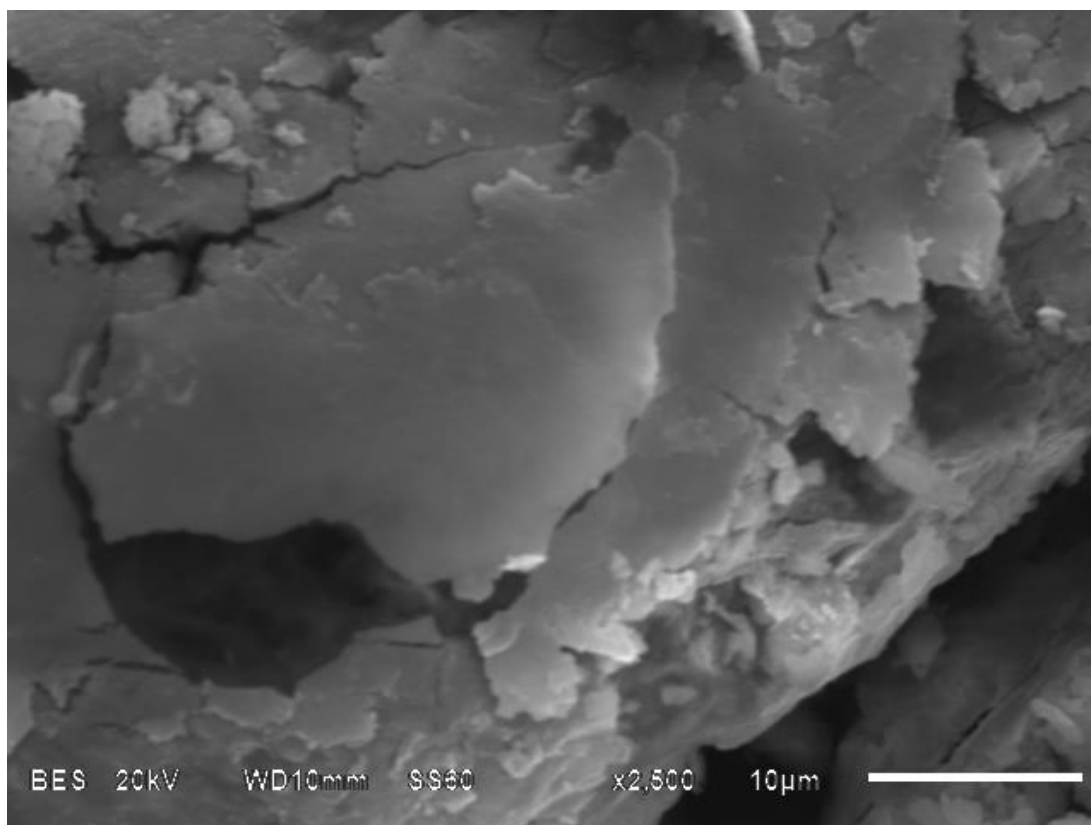
Figure 22 and Figure 23 showed an elongated void tubes structure for diatomaceous earth. These tubes contained a set of regular arrays of circular pores arranged along its assembly. Taking into account the microscale, circular pores are around 0.5 μm which is within the range of macroporous materials.
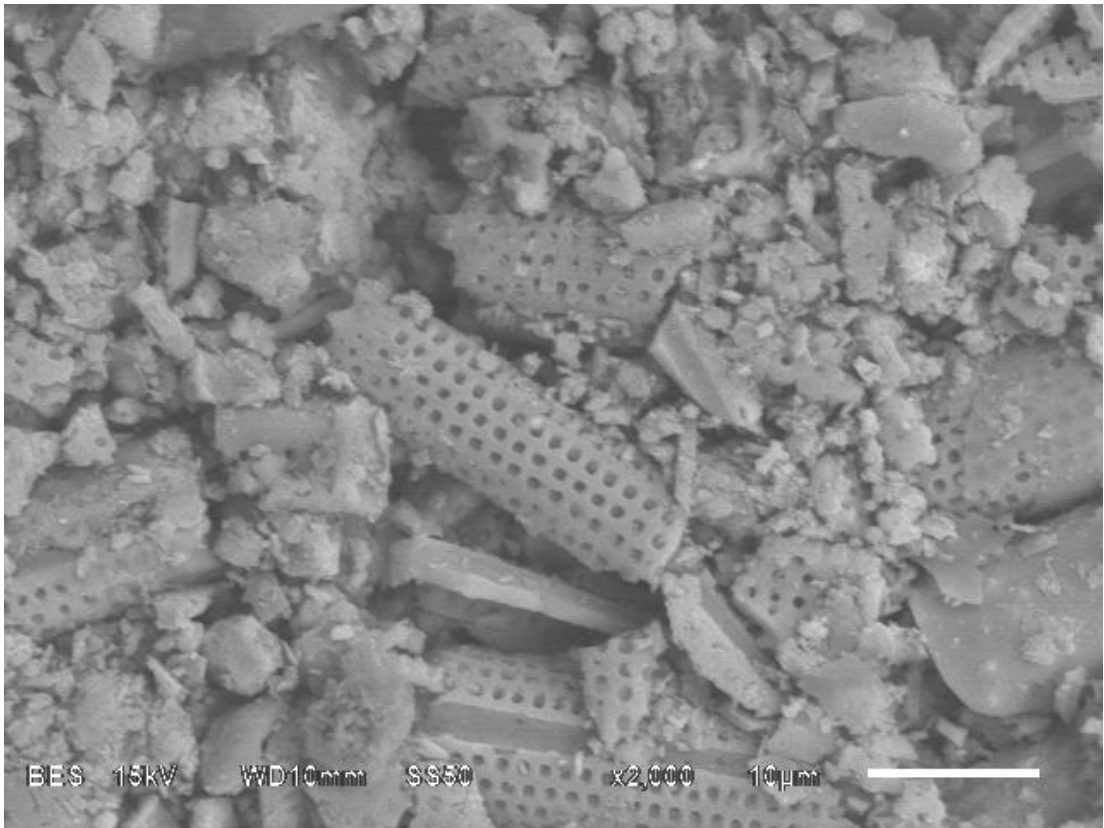
Figure 22. SEM micrography of natural diatomaceous earth (D).
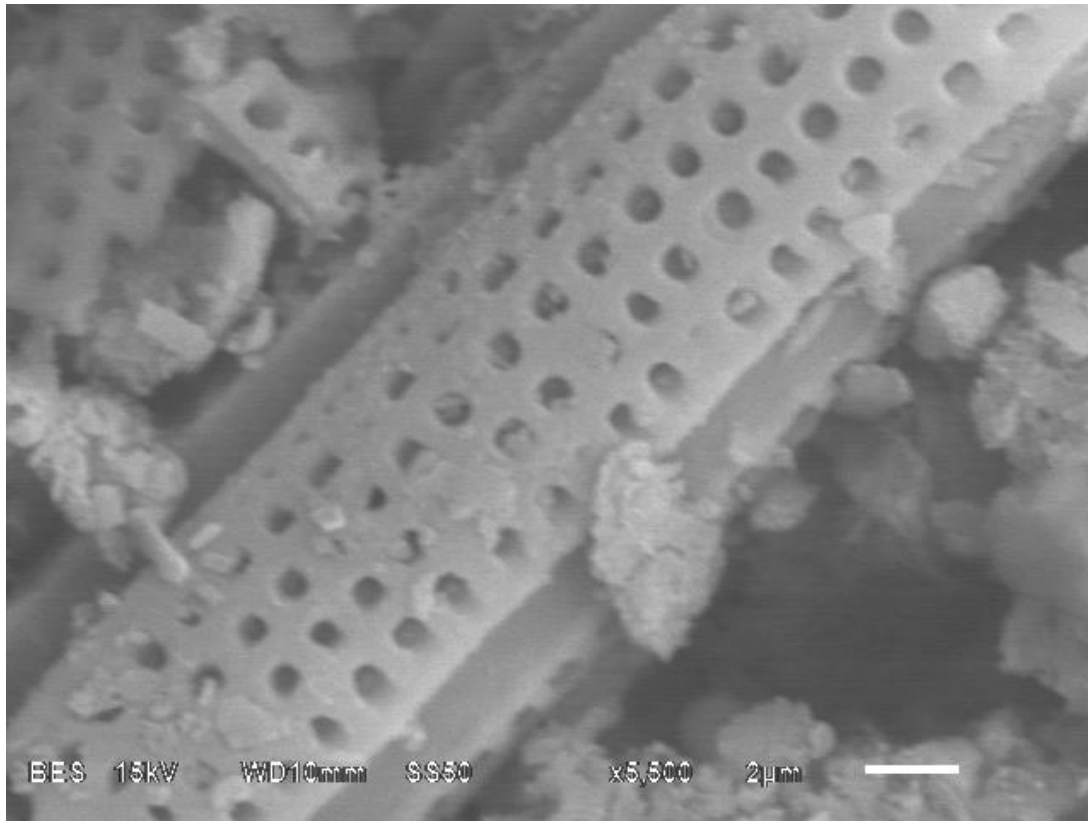
Figure 23. SEM micrography of natural diatomaceous earth (D). Magnification: x3500

According to Figure 24, Figure 25 and Figure 26 there is an evident change in morphology observed for composites prepared, with respect to of the starting material (M and D) that can be associated to the presence of chitosan. Composites surface (CM, CD and CMD) showed an integral, rough structure, and a good porous surface, which is suitable for allowing the metal ions diffusion through such structure during the adsorption process.

Figure 24. SEM micrography of composite CM.

Figure 25. SEM micrography of composite CD.

Figure 26. SEM micrography of composite CMD.

4.1.5 Ultraviolet-visible Spectroscopy

From equation obtained by Ni^{2+} calibration curve concentrations Ni^{2+} in solution after adsorption process were calculated.

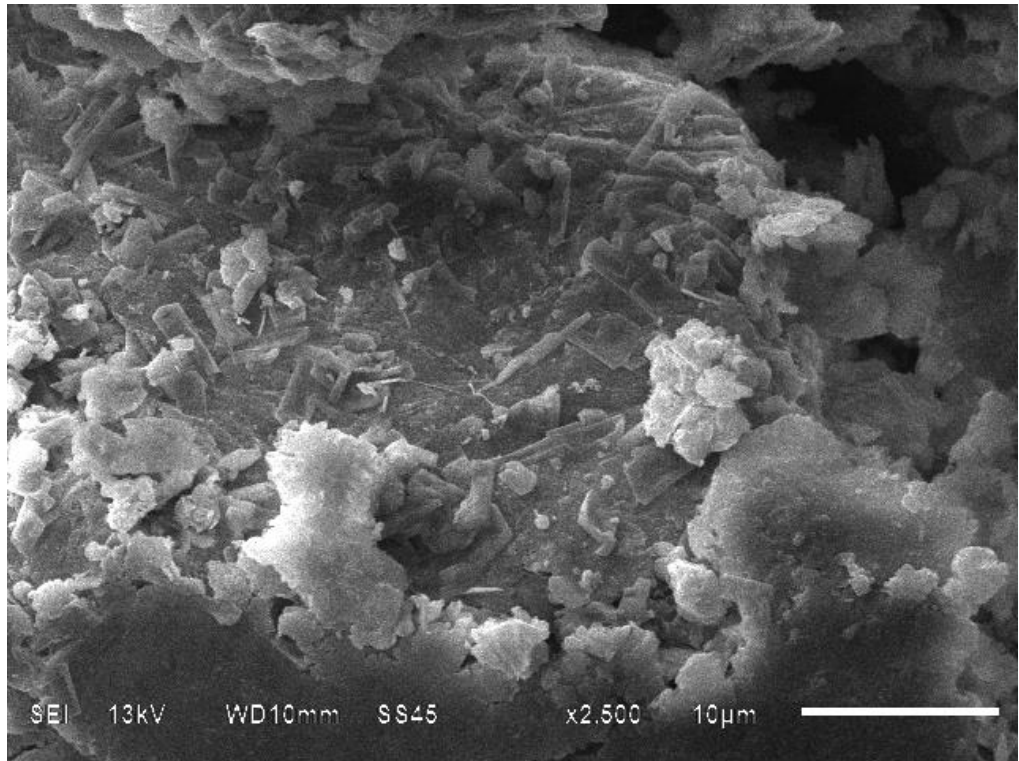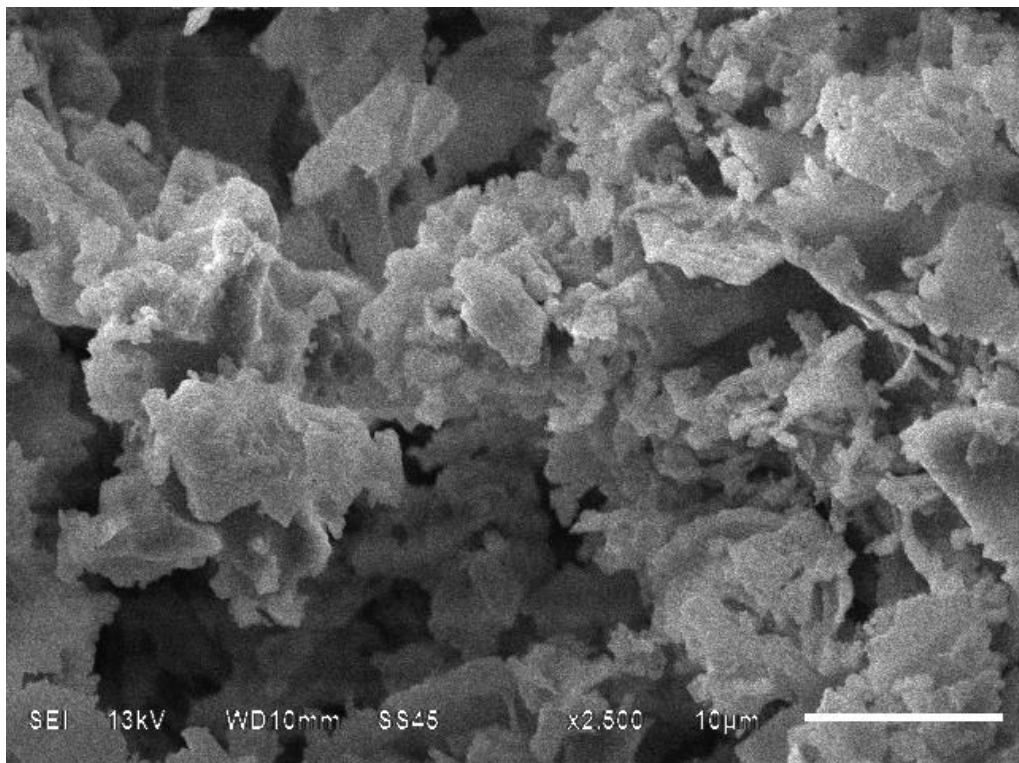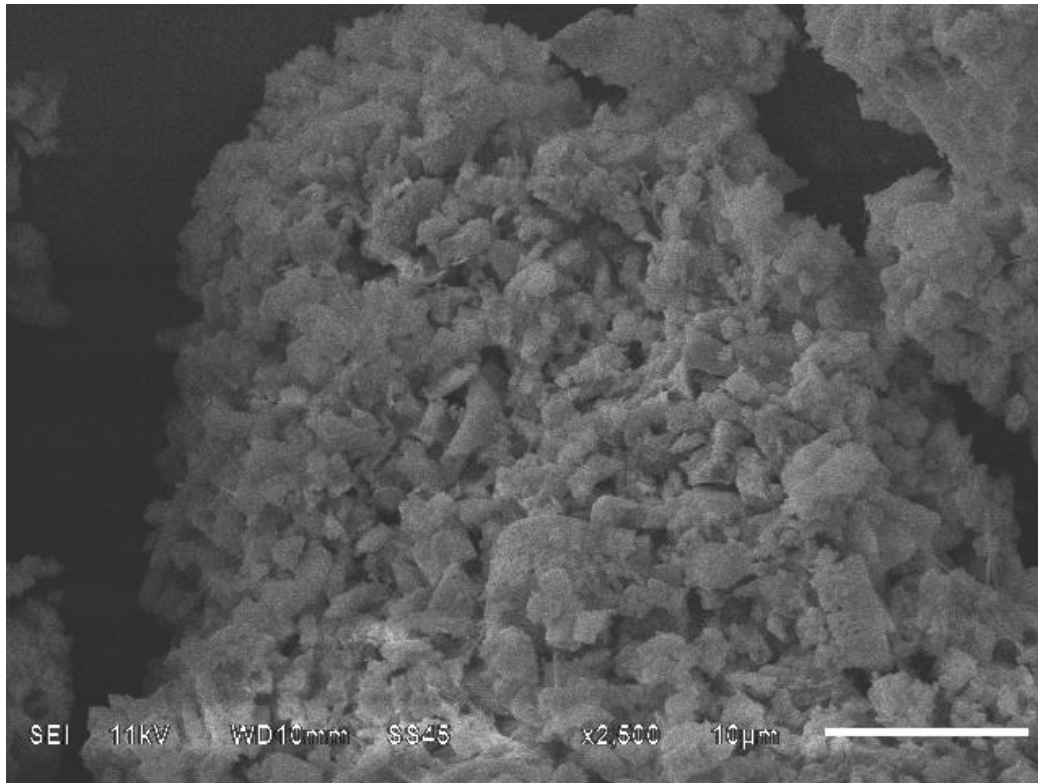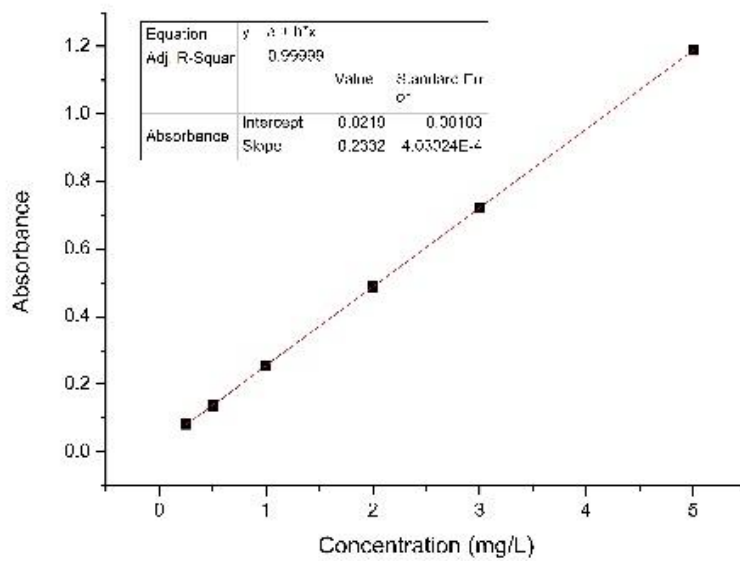Figure 27. Ni^{2+} calibration curve.

4.1.6 Brunauer- Emmett-Teller analysis

The specific BET areas of the studied adsorbents are reported in **Table 3.** Surface properties of adsorbents based on BET analysis . The Langmuir surface area of natural montmorillonite (M) and diatomaceous earth (D) were 22.86 and 1.80 m^2g^{-1}, respectively, which is within the range of reported values found in literature [28,75,76]. For montmorillonite clay composite (CM), it is observed a dramatically decrease in Langmuir surface area (comparing to parental M) with a value of 0,601 m^2g^{-1}. This behavior can be explained by the assumption that the chitosan can be obstructing the structural porosity of M. This assumption is supported by the fact that the micropore area for these materials decrease from of 0.64 to 0.056 m^2g^{-1}. On the contrary, for diatomaceous earth composite (CD), it is observed an increase of Langmuir surface area to 4.148 m^2g^{-1} which is not too large compared to other adsorbents, but it is enhanced when it is compared to pure chitosan (1.9 m^2g^{-1}). This behavior could be related to an increment in micropore area, from 0.22 to 0.43 m^2/g. The increment in the micropore are can be due to the chitosan cannot block the larger pores (macropores) of diatomaceous earth, instead the chitosan present inside the pores reduces the pore diameter producing meso and microporosity, therefore increasing the surface area. For CMD composite it is observed a considerable increment on the Langmuir surface area (74,14 m^2/g) compared to its parental materials. As pores of diatomaceous earth are larger than those present in montmorillonite clay it can be assumed the chitosan trends to enter in the macropore producing meso and microporosity, as suggested before, leading practically intact the microporosity of montmorillonite clay.

Table 3. Surface properties of adsorbents based on BET analysis

Adsorbent	Langmuir surface area (m^2/g)	Micropore area (m^2/g)	External surface area (m^2/g)
M	22.86	0.64	16.81
D	1.80	0.22	1.57
CM	0.601	0.056	0.357
CD	4.148	0.429	3.261
CMD	74,14	3.503	56.41

In all cases (parental materials and composites) a reversible type II isotherm was obtained. This result was expected because this type of isotherm describes non-porous or macroporous materials, as is the case of montmorillonite clay and diatomaceous

earth. Also, the adsorption isotherms show a hysteresis loop at medium-high relative pressure H2 type, which can be associated to empty spaces produced to stacking of laminar particles.
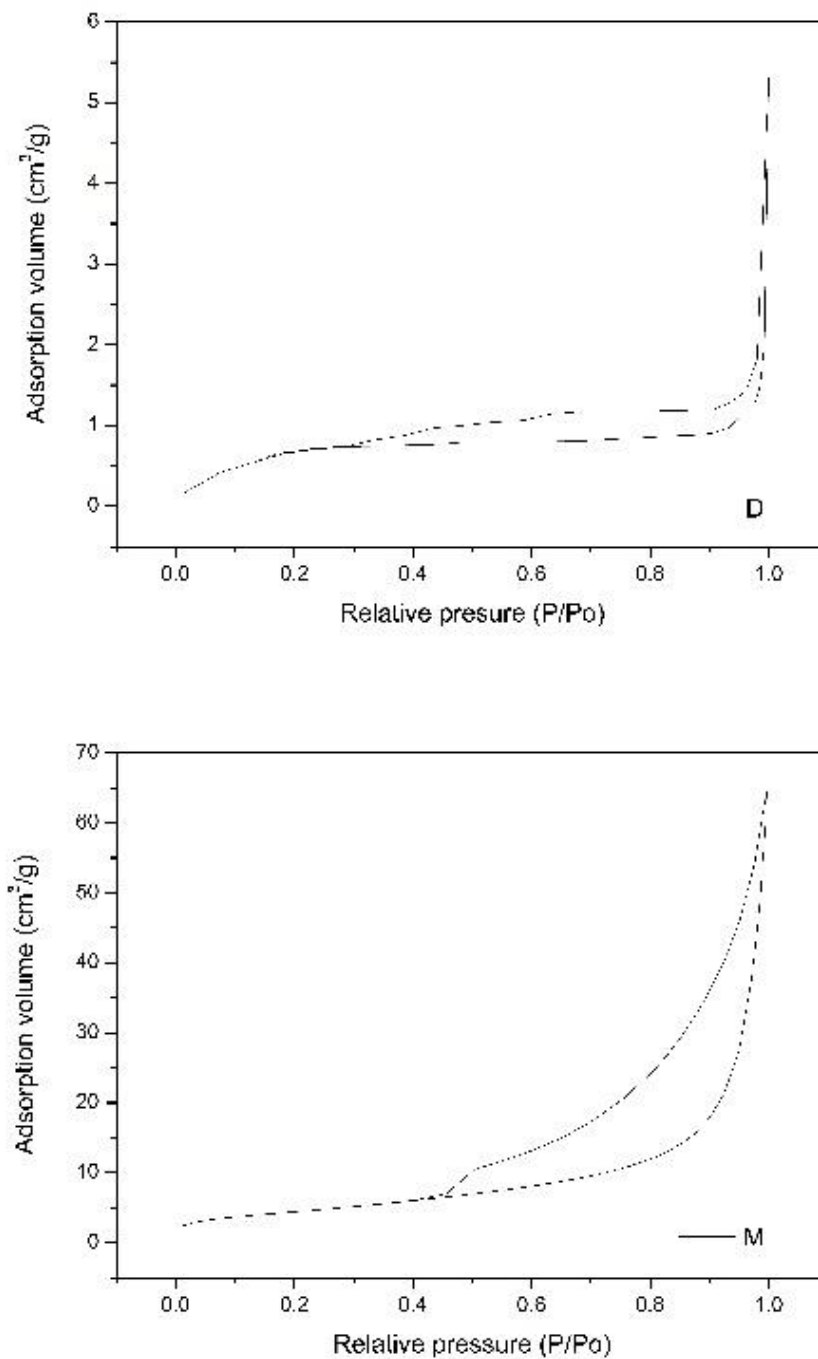

Figure 28. Nitrogen adsorption–desorption isotherms measured on natural
adsorbents; montmorillonite clay (M) and diatomaceous earth (D).
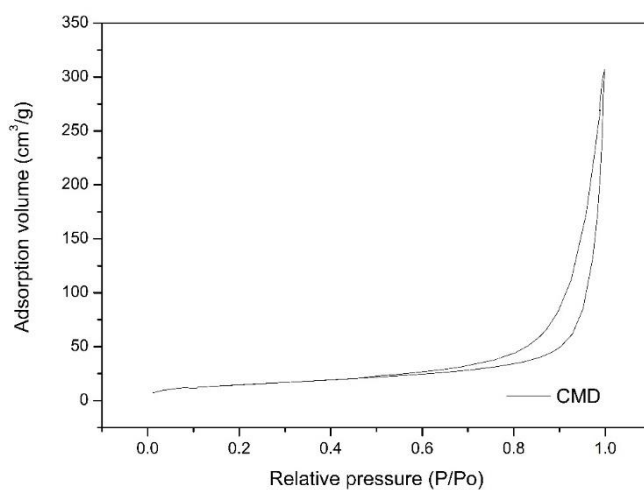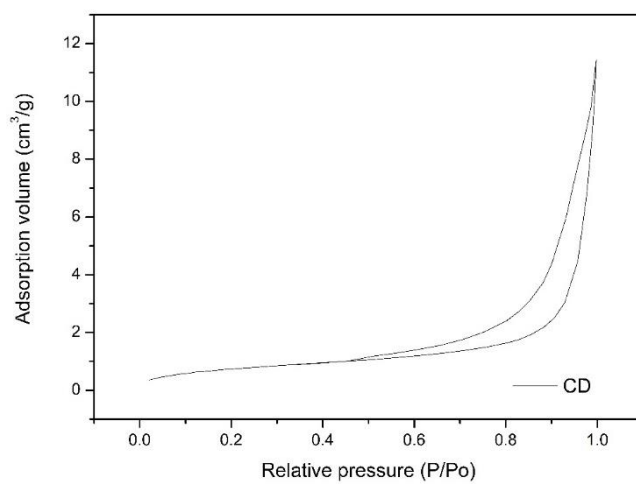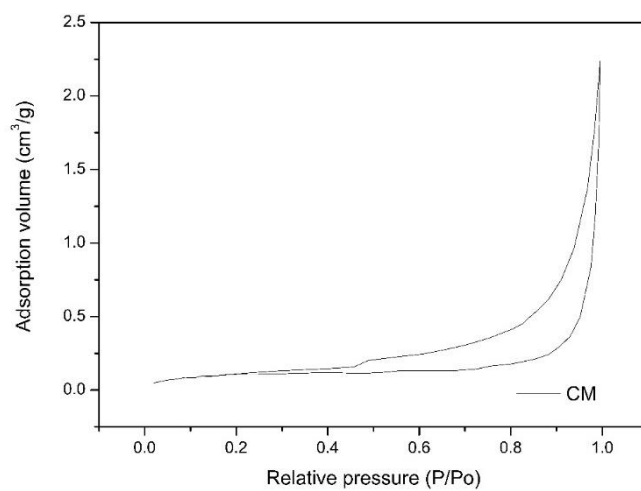
Figure 29. Nitrogen adsorption–desorption isotherms measured on synthesized composites CM, CD and CMD.

4.2 ADSORPTION STUDIES

4.2.1 Sorption dynamics

Ni^{2+} binding interactions with adsorbents depend on its properties in solution and the specific chemistry and morphology of the adsorbent surface. Then, it is necessary to analyze the effects of parameters like contact time, pH and initial Ni^{2+} concentration on the adsorption.

Effect of contact time

The effect of contact time on the sorption of Ni^{2+} onto M, D, CM, CD and CMD composites was investigated over different contact times: 1, 3 and 6 hours (Figure 25). From results, it is clear that there is no a huge difference in the adsorption capacity of adsorbents between the sets of contact times. Then, from this study it was selected 3 hours as the optimum contact time to reach the maximum sorption capacity.
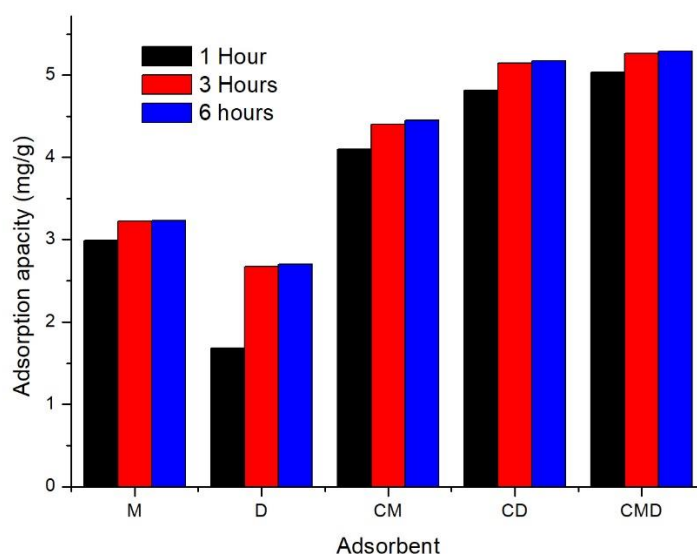
Figure 30. Effect of contact time

Effect of pH

The pH Ni^{2+} aqueous solutions affect the liquid-solid adsorption phenomena. It has been shown that surface charge, adsorption active sites of adsorbent, and interactions between Ni^{2+} and adsorbents are highly impacted by pH. Maximum Ni^{2+}

uptake onto M clay and D is 1.52 and 1.11 mg/g, respectively, at pH5.5. M and D mostly adsorb by hydroxyl functional groups (-OH) present on their surface [42]. In acidic conditions (pH=2) the presence of H^+ develops a strong competition between H^+ and Ni^{2+} ions for active adsorption sites [77], decreasing the Ni^{2+} uptake effectiveness. Moreover, the active sites on clay surface were demonstrated to be weakly acidic in nature [78,79] therefore, they gradually get more deprotonated as the pH increases thereby resulting in the observed higher adsorption of Ni^{2+}. Increasing pH (pH=9), sharply decreases the removal percentage due to the precipitation of Ni^{2+} in its hydroxyl form $Ni(OH)_2$ [2].

Chitosan composites (CM, CD and CMD) adsorb mostly by the electron pairs present in NH_2 functional groups [80]. At pH 5.5 it was reached the highest Ni^{+2} adsorption capacities of 1.76, 2.00 and 1,99 mg/g, for CM, CD and CMD respectively. When pH was increased to 9, the removal capacity of adsorbents decreased due to the precipitation of nickel hydroxide in the solution as explained before. On the other hand, when pH was decreased to 2, the removal capacity of adsorbents also decreased due to the protonation of chitosan amine groups (-NH_2) obtaining NH_4^+, this makes the surface of chitosan composites beads become positively charged, causing a columbic repulsion between Ni^{2+} and the protonated amino group on the surface of the composites. Then, when the amine groups are completely deprotonated from NH_4^+ to (-NH_2), a large mass of active adsorption sites are available for the adsorption of Ni^{2+} by electrostatic attraction and they become ready to bond and/or coordinate with the Ni^{2+}. Hence, the adsorption process onto composite beads is mainly controlled by electrostatic attraction between the positive charge of Ni^{2+} ions and the electron pairs on the nitrogen atoms (-NH_2).
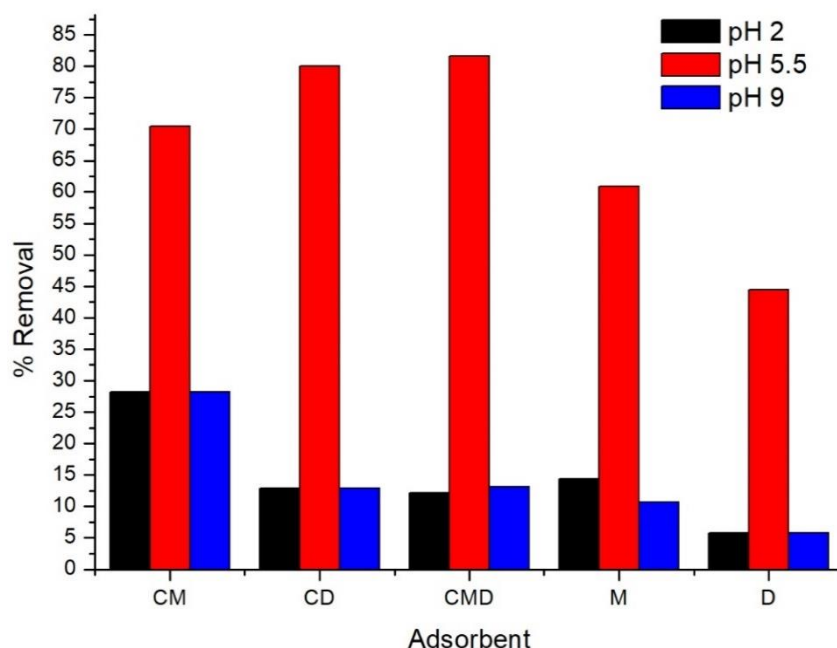
Figure 31. Effect of pH on adsorption.

Effect of initial metal ion concentration

As presented in Figure 32, the adsorption capacity of adsorbents increase proportionally, with the initial concentration for all the adsorbents (M, D, CM, CD and CMD). However, the maximum removal efficiency at equilibrium decreases significantly as result of increasing concentration from 0.25 to 5 mg/L as shown in Figure 33. These opposite behaviors between removal efficiency and adsorption capacity are associated to the fact that, at high Ni^{2+} concentration, the number of ions of Ni^{2+} reaching the adsorbent active sites increased resulting in higher probability of interaction between Ni^{2+} and adsorbent surface, thereby increasing the adsorption capacity. On the other hand, it was expected that there would be an increase in the ratio of the number Ni^{2+} in solution to the available number of adsorption sites as the initial metal ions increase in solution. Thus, this created a competitive environment which was vulnerable to reducing the overall removal efficiency.

Figure 32. Adsorption capacity vs Initial metal ion concentration

Figure 33. Removal efficiency vs Initial metal ion concentration

4.2.2 Adsorption isotherms

Freundlich model effectively fits the experimental data as well as Langmuir model (**Table 4**) for all adsorbents used in this investigation (M, D, CM, CD and CDM). The R^2 values indicated in the **Table 4** are very close to the unit demonstrating the strong correlation with both models (Figure 34). This could be related to two different types of binding sites. One of them might be associated to weak functional groups, m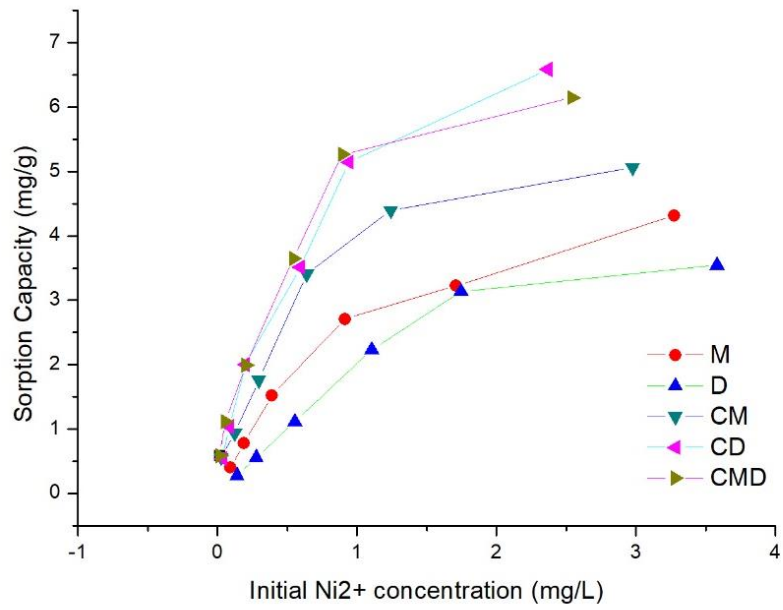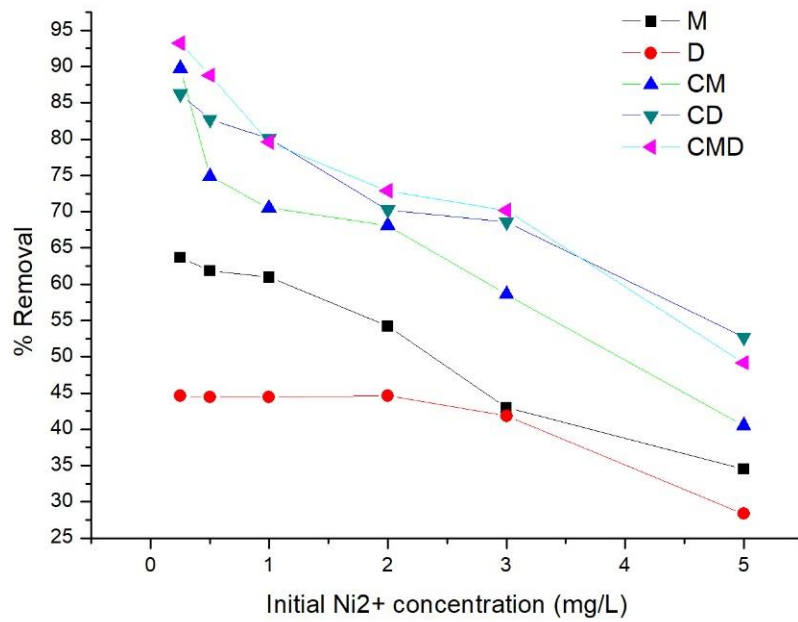eanwhile, the other can be associated with strong functional groups present on adsorbents surface. The weak binding sites can be associated to heterogeneous surface and reversible adsorption while strong binding sites to homogeneous surface adsorption and formation of a monolayer (chemisorption). The values of the Freundlich parameter n were found to be greater than 1, which suggested favorable uptake of the adsorbate by parental materials (M and D) and composites (CM, CD and CMD).

The maximum capacity of adsorption of parental materials M and D were 5.82 and 1.66 mg/g, respectively. M shows a better maximum adsorption capacity due to more active hydroxyl groups present in its surface while, D shows a very low adsorption capacity because of lower amount and weaker silanol groups. The later statement is supported by the high crystallinity shown by its XRD pattern. The maximum capacity of adsorption (Qm (mg/g)) were enhanced in composites. This fact can be explained by the presence of functional groups such as amine (-NH$_2$) and hydroxyl (-OH) which may serve as coordination sites to form complexes with Ni^{2+} metal ion. There is a slight increase on the Qm from M to CM. Which can be thought that there should be a decrease in Qm due to the blocking of the structural porosity of M (supported by BET analysis), however the functional groups in chitosan remain available and the adsorption capacity of the CM could be associated to this functional groups. In case of Qm for D and CD, there is a marked increment in the composite sample. This result is associated to the meso and microporosity created, which increases the surface area and lead to a higher exposure of functional groups of chitosan.

Table 4. Values obtained of the parameters of Langmuir and Freundlich models

Adsorption isotherm	Parameter	Adsorbent				
		M	D	CM	CD	CDM
Langmuir	Q_m (mg/g)	5.82	1.66	5.95	8.64	6.95
	K_L (L/mg)	0.84	0.36	1.961	2.212	2.862
	R_L	0.34-0.63	0.36-0.91	0.13-0.74	0.08-0.64	0.07-0.58
	R^2	0.9907	0.8568	0.9782	0.9869	0.9829
Freundlich	K_F	2.343	1.660	3.425	4.833	0.9829
	n (l/mg)	1.503	1.204	1.947	2.460	2.013
	R^2	0.9658	0.9625	0.9601	0.9827	0.9825
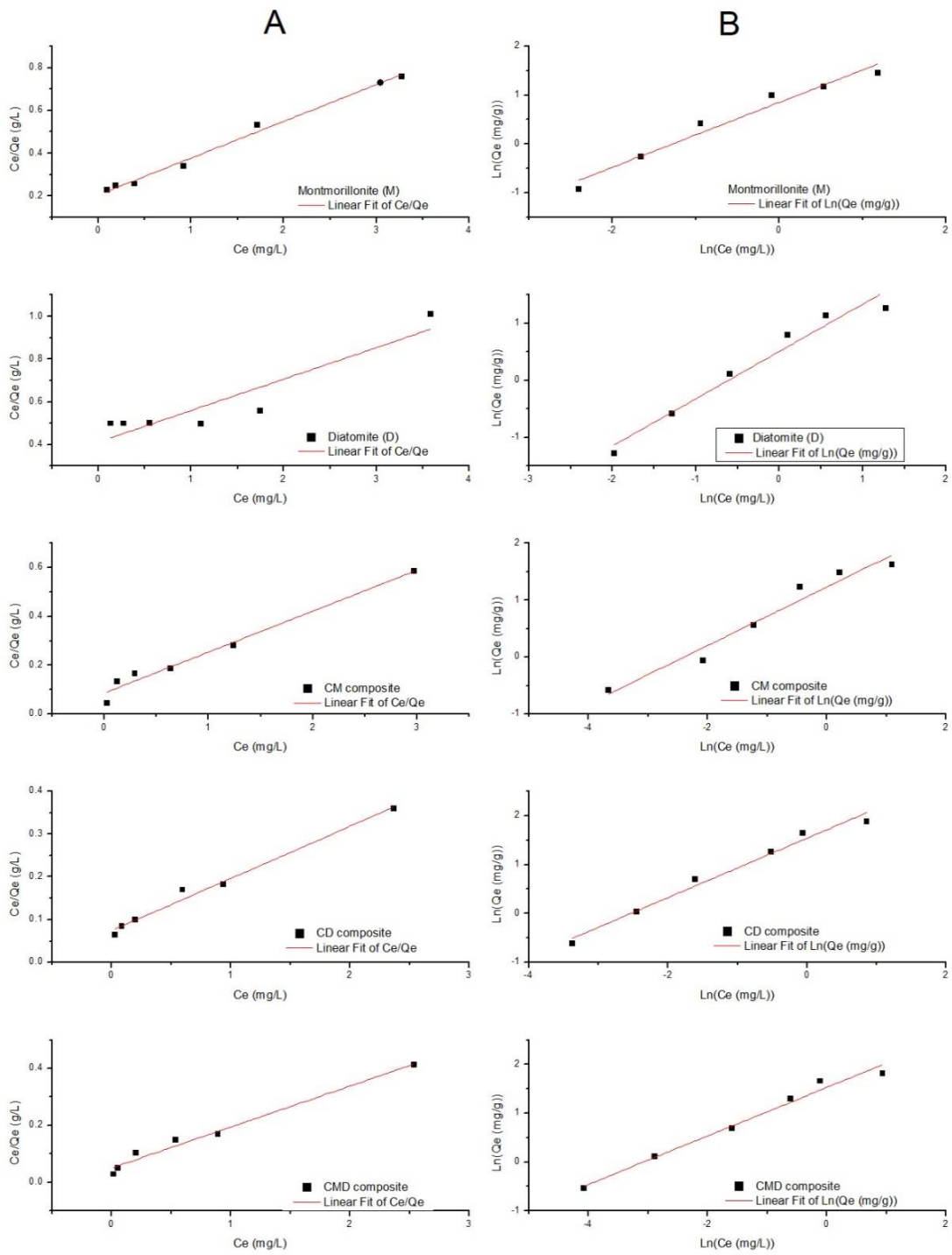
Figure 34. Adsorption isotherms. Column A shows the Langmuir model and column B shows the Freundlich model for different adsorbents.

4.3 ADSORPTION CHARACTERIZATION

Characterization techniques such as SEM and EDS were used to ensure adsorption on Ni^{2+} onto natural and synthesized adsorbents

Energy Dispersive x-ray Spectroscopy (EDS) was used to confirm the adsorption of Ni(II) onto CM, CD and CMD composites and to determine the weight percentages of this metal ions (Table 5).

Table 5. Weight percentage of elemental composition obtained of EDS analysis

	CM	CD	CDM
Na	3.66	8.87	7.94
Mg	2.52		1.99
Al	18.55	2.26	
Si	58.23	82	85.41
K	1.01		
Fe	13.44	1.82	
Ni	2.59	0.87	3.67

The surface of the loaded adsorbents (CM, CD, CMD) is altered to less porous and adsorbed metal ions formed a bright thin layer on the surface that confirms the adsorption of the Ni^{2+} metal ions onto composites.

Figure 35. SEM images of CM, CD and CMD after adsorption process.

Chapter 5: Conclusions

In this study, it was successfully prepared montmorillonite clay/chitosan (CM). diatomaceous earth/chitosan (CD) and montmorillonite clay/diatomaceous earth/chitosan (CDM) composites in a spherical shape by drop wise method. These synthesized materials are a low-cost alternative adsorbent for Ni^{2+} removal from aqueous solution. Chitosan was coated ont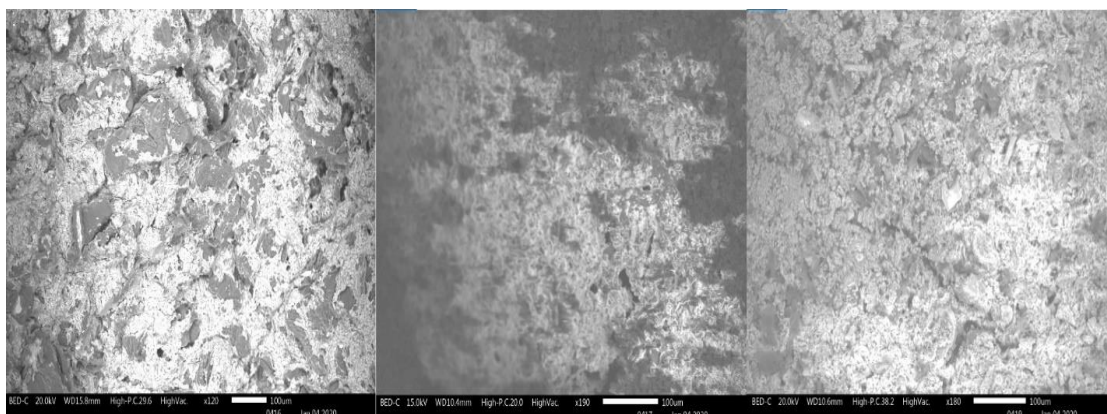o the diatomaceous earth and montmorillonite clay to enhance its adsorption capacity and to increase the accessibility of the binding sites. In order to stablish an adsorption mechanism, parental materials and composites were characterized by DRX, SEM, EDS, FTIR and BET. Adsorption reached equilibrium in about 3 hours and it was highly depended on the initial metal concentration and solution-pH. The optimum pH was found 5.5 for Ni^{2+} adsorption. Langmuir and Freundlich isotherms models were found to fit the experimental data because of the presence of two types of binding sites. Under optimal conditions, the maximal adsorption capacities of adsorbents based on the Langmuir isotherm model were 5.82, 1.66, 5.95, 8.64 and 6.95 for M, D, CM, CD and CMD respectively. There is synergistic effect between precursors of composites because an enhancement in the maximal adsorption capacities of composites compared to that of the precursor materials were found. The aforementioned results established that the synthesized composites can be used confidently as the promising and cost-effective adsorbent for Ni^{2+} removal from the industrial wastewater. The most optimal combination was found to be composite CD as it shows the best adsorption capacity.

Chapter 6: Recommendations

For further studies, it is suggested to evaluate other parameters affecting the adsorption process in order to work in optimal conditions. Also, it is important to obtain adsorption kinetics and thermodynamic parameters. Investigate the adsorption-desorption cycles. Competitive adsorption studies between other heavy metals or combination of them should be investigated too.

Bibliography

(1)   Verma, R.; Dwivedi, P. Heavy Metal Water Pollution- A Case Study. *Recent Res. Sci. Technol.* **2013**.

(2)   Barakat, M. A. New Trends in Removing Heavy Metals from Industrial Wastewater. *Arabian Journal of Chemistry*. 2011. https://doi.org/10.1016/j.arabjc.2010.07.019.

(3)   Oliveira Da Silva, A. L.; Barrocas, P. R. G.; Do Couto Jacob, S.; Moreira, J. C. Dietary Intake and Health Effects of Selected Toxic Elements. *Brazilian Journal of Plant Physiology*. 2005. https://doi.org/10.1590/s1677-04202005000100007.

(4)   Harari, R.; Harari, F.; Forastiere, F. Environmental Nickel Exposure from Oil Refinery Emissions: A Case Study in Ecuador. *Ann. Ist. Super. Sanita* **2016**. https://doi.org/10.4415/ANN_16_04_06.

(5)   Babel, S.; Kurniawan, T. A. Low-Cost Adsorbents for Heavy Metals Uptake from Contaminated Water: A Review. *Journal of Hazardous Materials*. 2003. https://doi.org/10.1016/S0304-3894(02)00263-7.

(6)   Salih, S. S.; Ghosh, T. K. Highly Efficient Competitive Removal of Pb(II) and Ni(II) by Chitosan/Diatomaceous Earth Composite. *J. Environ. Chem. Eng.* **2018**. https://doi.org/10.1016/j.jece.2017.12.037.

(7)   Chaplin, M. F. Water: Its Importance to Life. *Biochem. Mol. Biol. Educ.* **2001**. https://doi.org/10.1016/S1470-8175(01)00017-0.

(8)   Petrucci, R. H.; Harwood, W. S.; Herring, G. E.; Madura, J. *General Chemistry: Principles & Modern Applications*; 2013. https://doi.org/10.1017/CBO9781107415324.004.

(9)   Carbonaro, R. F. Water Chemistry. In *Introduction to Environmental Management*; 2009. https://doi.org/10.1201/noe0849398438.ch83.

(10)   Bralower, T.; Bice, D. Distribution of Water on the Earth's Surface https://www.e-education.psu.edu/earth103/node/701.

(11)   Denchak, M. Water Pollution: Everything You Need to Know

https://www.nrdc.org/stories/water-pollution-everything-you-need-know.

(12)   Muralikrishna, I. V.; Manickam, V. Introduction. In *Environmental Management*; 2017. https://doi.org/10.1016/b978-0-12-811989-1.00001-4.

(13)   Alo, B. List of Water Pollutants https://sciencing.com/list-water-pollutants-6309497.html.

(14)   Gakwisiri, C.; Raut, N.; Al-Saadi, A.; Al-Aisri, S.; Al-Ajmi, A. A Critical Review of Removal of Zinc from Wastewater. In *Lecture Notes in Engineering and Computer Science*; 2012.

(15)   Crini, G.; Lichtfouse, E.; Wilson, L. D.; Morin-Crini, N. Adsorption-Oriented Processes Using Conventional and Non-Conventional Adsorbents for Wastewater Treatment; 2018. https://doi.org/10.1007/978-3-319-92111-2_2.

(16)   Jaishankar, M.; Tseten, T.; Anbalagan, N.; Mathew, B. B.; Beeregowda, K. N. Toxicity, Mechanism and Health Effects of Some Heavy Metals. *Interdisciplinary Toxicology*. 2014. https://doi.org/10.2478/intox-2014-0009.

(17)   Cempel, M.; Nikel, G. Nickel: A Review of Its Sources and Environmental Toxicology. *Polish Journal of Environmental Studies*. 2006.

(18)   Parmar, M.; Singh Thakur, L. HEAVY METAL CU, NI AND ZN: TOXICITY, HEALTH HAZARDS AND THEIR REMOVAL TECHNIQUES BY LOW COST ADSORBENTS: A SHORT OVERVIEW. *Int. J. Plant, Anim. and, Environ. Sci.* **2013**.

(19)   Ahmed, A. M.; Ali, A. E.; Ghazy, A. H. Adsorption Separation of Nickel from Wastewater by Using Olive Stones. *Adv. J. Chem. A* **2019**, *2* (1), 79–93. https://doi.org/10.29088/sami/ajca.2019.2.7993.

(20)   Dhingra, N.; Singh, N. S.; Parween, T.; Sharma, R. Heavy Metal Remediation by Natural Adsorbents. In *Modern Age Waste Water Problems*; 2020. https://doi.org/10.1007/978-3-030-08283-3_10.

(21)   United Nations Children Fund; World health Organisation. *Progress on Drinking Water, Sanitation and Hygiene*; 2017. https://doi.org/10.1111 / tmi.12329.

(22)   Norma Técnica Ecuatoriana. Agua Potable. Requisitos. Nte Inen 1108. *Inst.*

Ecuatoriano Norm. **2014**.

(23) CONSTITUCION DEL ECUADOR. Constitución Del Ecuador - 2008. *Regist. Of.* **2008**.

(24) Kurniawan, T. A.; Chan, G. Y. S.; Lo, W. H.; Babel, S. Physico-Chemical Treatment Techniques for Wastewater Laden with Heavy Metals. *Chem. Eng. J.* **2006**. https://doi.org/10.1016/j.cej.2006.01.015.

(25) Gunatilake, S. K. Methods of Removing Heavy Metals From. *J. Multidiscip. Eng. Sci. Stud. Ind. Wastewater* **2015**.

(26) Kazemimoghadam, M.; Mohammadi, T. Separation of Water/UDMH Mixtures Using Hydroxysodalite Zeolite Membranes. *Desalination* **2005**. https://doi.org/10.1016/j.desal.2005.02.010.

(27) Barakat, M. A.; Chen, Y. T.; Huang, C. P. Removal of Toxic Cyanide and Cu(II) Ions from Water by Illuminated TiO 2 Catalyst. *Appl. Catal. B Environ.* **2004**. https://doi.org/10.1016/j.apcatb.2004.05.003.

(28) Sen Gupta, S.; Bhattacharyya, K. G. Adsorption of Heavy Metals on Kaolinite and Montmorillonite: A Review. *Physical Chemistry Chemical Physics*. 2012. https://doi.org/10.1039/c2cp40093f.

(29) Weber, W. J. Adsorption Processes. *Pure Appl. Chem.* **1974**. https://doi.org/10.1351/pac197437030375.

(30) Crini, G.; Lichtfouse, E.; Wilson, L. D.; Morin-Crini, N. Conventional and Non-Conventional Adsorbents for Wastewater Treatment. *Environmental Chemistry Letters*. 2019. https://doi.org/10.1007/s10311-018-0786-8.

(31) Gaspard, J. P. Physisorption and Chemisorption. In *Interfacial Aspects of Phase Transformations*; 1982. https://doi.org/10.1007/978-94-009-7870-6_4.

(32) Helfferich, F. G.; Hwang, Y. L. Ion Exchange Kinetics. In *Ion Exchangers*; 2011. https://doi.org/10.1515/9783110862430.1277.

(33) Guggenheim, S.; Martin, R. T.; Alietti, A.; Drits, V. A.; Formoso, M. L. L.; Galán, E.; Köster, H. M.; Morgan, D. J.; Paquet, H.; Watanabe, T.; Bain, D. C.; Ferrell, R. E.; Bish, D. L.; Fanning, D. S.; Guggenheim, S.; Kodama, H.; Wicks, F. J. Definition of Clay and Clay Mineral: Joint Report of the AIPEA

Nomenclature and CMS Nomenclature Committees. *Clays and Clay Minerals.* 1995. https://doi.org/10.1346/CCMN.1995.0430213.

(34)   Egger, A. The Silicate Minerals https://www.visionlearning.com/en/library/Earth-Science/6/The-Silicate-Minerals/140.

(35)   Nelson, S. Phyllosilicates (Sheet Silicates) https://www.tulane.edu/~sanelson/eens211/phyllosilicates.htm.

(36)   Besoain, E. *Mineralogía de Arcillas de Suelos.*; 1985.

(37)   Gu, S.; Kang, X.; Wang, L.; Lichtfouse, E.; Wang, C. Clay Mineral Adsorbents for Heavy Metal Removal from Wastewater: A Review. *Environ. Chem. Lett.* **2018**. https://doi.org/10.1007/s10311-018-0813-9.

(38)   Phyllosilicates.

(39)   Rautureau, M.; Gomes, C. de S. F.; Liewig, N.; Katouzian-Safadi, M. *Clays and Health: Properties and Therapeutic Uses*; 2017. https://doi.org/10.1007/978-3-319-42884-0.

(40)   Zarzycki, P.; Szabelski, P.; Piasecki, W. Modelling of ζ-Potential of the Montmorillonite/Electrolyte Solution Interface. *Appl. Surf. Sci.* **2007**. https://doi.org/10.1016/j.apsusc.2006.12.060.

(41)   Zarzycki, P.; Thomas, F. Theoretical Study of the Acid-Base Properties of the Montmorillonite/Electrolyte Interface: Influence of the Surface Heterogeneity and Ionic Strength on the Potentiometric Titration Curves. *J. Colloid Interface Sci.* **2006**. https://doi.org/10.1016/j.jcis.2006.06.044.

(42)   Bhattacharyya, K. G.; Gupta, S. Sen. Adsorption of a Few Heavy Metals on Natural and Modified Kaolinite and Montmorillonite: A Review. *Advances in Colloid and Interface Science*. 2008. https://doi.org/10.1016/j.cis.2007.12.008.

(43)   Alexander, J. A.; Ahmad Zaini, M. A.; Surajudeen, A.; Aliyu, E. N. U.; Omeiza, A. U. Surface Modification of Low-Cost Bentonite Adsorbents—A Review. *Particulate Science and Technology*. 2019. https://doi.org/10.1080/02726351.2018.1438548.

(44)   Smol, J. P.; Stoermer, E. F. *The Diatoms: Applications for the Environmental*

and Earth Sciences, Second Edition; 2010.
https://doi.org/10.1017/CBO9780511763175.

(45)   Calvert, R. Diatomaceous Earth. *Journal of Chemical Education*. 1930.
https://doi.org/10.1021/ed007p2829.

(46)   Schüth, F.; Schmidt, W. Microporous and Mesoporous Materials. *Adv. Mater.*
2002. https://doi.org/10.1002/1521-4095(20020503)14:9<629::AID-
ADMA629>3.0.CO;2-B.

(47)   Al-Ghouti, M. A.; Khraisheh, M. A. M.; Allen, S. J.; Ahmad, M. N. The
Removal of Dyes from Textile Wastewater: A Study of the Physical
Characteristics and Adsorption Mechanisms of Diatomaceous Earth. *J.
Environ. Manage.* **2003**. https://doi.org/10.1016/j.jenvman.2003.09.005.

(48)   Yuan, P.; Wu, D. Q.; He, H. P.; Lin, Z. Y. The Hydroxyl Species and Acid
Sites on Diatomite Surface: A Combined IR and Raman Study. *Appl. Surf. Sci.*
2004. https://doi.org/10.1016/j.apsusc.2003.10.031.

(49)   Daifullah, A. A. M.; Awwad, N. S.; El-Reefy, S. A. Purification of Wet
Phosphoric Acid from Ferric Ions Using Modified Rice Husk. *Chem. Eng.
Process. Process Intensif.* **2004**. https://doi.org/10.1016/S0255-
2701(03)00014-X.

(50)   Islam, S.; Bhuiyan, M. A. R.; Islam, M. N. Chitin and Chitosan: Structure,
Properties and Applications in Biomedical Engineering. *Journal of Polymers
and the Environment*. 2017. https://doi.org/10.1007/s10924-016-0865-5.

(51)   Ravi Kumar, M. N. V. A Review of Chitin and Chitosan Applications.
Reactive and Functional Polymers. 2000. https://doi.org/10.1016/S1381-
5148(00)00038-9.

(52)   Rinaudo, M. Chitin and Chitosan: Properties and Applications. *Progress in
Polymer Science (Oxford)*. 2006.
https://doi.org/10.1016/j.progpolymsci.2006.06.001.

(53)   Freundlich, H. Über Die Adsorption in Lösungen. *Zeitschrift für Phys. Chemie*
2017. https://doi.org/10.1515/zpch-1907-5723.

(54)   Langmuir, I. The Adsorption of Gases on Plane Surfaces of Glass, Mica and
Platinum. *J. Am. Chem. Soc.* **1918**. https://doi.org/10.1021/ja02242a004.

(55) Bunaciu, A. A.; Udriştioiu, E. gabriela; Aboul-Enein, H. Y. X-Ray Diffraction: Instrumentation and Applications. *Critical Reviews in Analytical Chemistry*. 2015. https://doi.org/10.1080/10408347.2014.949616.

(56) Malayoglu, U. Removal of Heavy Metals by Biopolymer (Chitosan)/Nanoclay Composites. *Sep. Sci. Technol.* **2018**. https://doi.org/10.1080/01496395.2018.1471506.

(57) Teppola, P. Near-Infrared Spectroscopy, Principles, Instruments, Applications. *J. Chemom.* **2002**.

(58) Lloyd, D. R. The Infrared Spectra of Minerals. *Anal. Chim. Acta* **1975**. https://doi.org/10.1016/s0003-2670(00)00181-1.

(59) Physical Principles of Electron Microscopy. *Mater. Today* **2005**. https://doi.org/10.1016/s1369-7021(05)71290-6.

(60) Stokes, D. J. *Principles and Practice of Variable Pressure/Environmental Scanning Electron Microscopy (VP-ESEM)*; 2008. https://doi.org/10.1002/9780470758731.

(61) Rakhee; Mishra, J.; Sharma, R. K.; Misra, K. Characterization Techniques for Herbal Products. In *Management of High Altitude Pathophysiology*; 2018. https://doi.org/10.1016/B978-0-12-813999-8.00009-4.

(62) Thermo Spectronic. Basic UV-Vis Theory , Concepts and Applications Basic. *ThermoSpectronic* **2013**.

(63) Zielinski, J. M.; Kettle, L. Physical Characterization : Surface Area and Porosity. *Intertek Chem. Pharamaceuticals* **2013**.

(64) Bergadà Miró, O. *Diseño de Catalizadores Para Una Obtención Limpia de 2-Feniletanol. Parte Experimental*; 2007.

(65) Lowell, S.; Shields, J. E.; Lowell, S.; Shields, J. E. Adsorption Isotherms. In *Powder Surface Area and Porosity*; 1991. https://doi.org/10.1007/978-94-015-7955-1_3.

(66) Keller, J. U.; Staudt, R. *Gas Adsorption Equilibria: Experimental Methods and Adsorptive Isotherms*; 2005. https://doi.org/10.1007/b102056.

(67) Sultan, M.; Miyazaki, T.; Koyama, S. Optimization of Adsorption Isotherm

Types for Desiccant Air-Conditioning Applications. *Renew. Energy* **2018**. https://doi.org/10.1016/j.renene.2018.01.045.

(68) Akpomie, K. G.; Dawodu, F. A. Acid-Modified Montmorillonite for Sorption of Heavy Metals from Automobile Effluent. *Beni-Suef Univ. J. Basic Appl. Sci.* **2016**. https://doi.org/10.1016/j.bjbas.2016.01.003.

(69) Mineralogy Database. *Choice Rev. Online* **2007**. https://doi.org/10.5860/choice.45-0296.

(70) Yang, S.; Ren, X.; Zhao, G.; Shi, W.; Montavon, G.; Grambow, B.; Wang, X. Competitive Sorption and Selective Sequence of Cu(II) and Ni(II) on Montmorillonite: Batch, Modeling, EPR and XAS Studies. *Geochim. Cosmochim. Acta* **2015**, *166* (February 2018), 129–145. https://doi.org/10.1016/j.gca.2015.06.020.

(71) Kumar, S.; Koh, J.; Kim, H.; Gupta, M. K.; Dutta, P. K. A New Chitosan-Thymine Conjugate: Synthesis, Characterization and Biological Activity. *Int. J. Biol. Macromol.* **2012**. https://doi.org/10.1016/j.ijbiomac.2012.01.015.

(72) Salih, S. S.; Ghosh, T. K. Preparation and Characterization of Chitosan-Coated Diatomaceous Earth for Hexavalent Chromium Removal. *Environ. Process.* **2018**. https://doi.org/10.1007/s40710-017-0280-5.

(73) Pereira, M. A.; Vasconcelos, D. C. L.; Vasconcelos, W. L. Synthetic Aluminosilicates for Geopolymer Production. *Mater. Res.* **2019**. https://doi.org/10.1590/1980-5373-MR-2018-0508.

(74) Wei, X.; Wang, W.; Xiao, J.; Zhang, L.; Chen, H.; Ding, J. Hierarchically Porous Aluminosilicates as the Water Vapor Adsorbents for Dehumidification. *Chem. Eng. J.* **2013**. https://doi.org/10.1016/j.cej.2013.05.062.

(75) Rodríguez, Y. M. V.; Beltrán, H. I.; Vázquez-Labastida, E.; Linares-López, C.; Salmón, M. Synthesis and Characterization of Montmorillonite Clays with Modulable Porosity Induced with Acids and Superacids. *J. Mater. Res.* **2007**. https://doi.org/10.1557/jmr.2007.0098.

(76) Wypych, G. FILLERS – ORIGIN, CHEMICAL COMPOSITION, PROPERTIES, AND MORPHOLOGY. In *Handbook of Fillers*; 2016. https://doi.org/10.1016/b978-1-895198-91-1.50004-x.

(77)   Pham, T. D.; Do, T. T.; Ha, V. L.; Doan, T. H. Y.; Nguyen, T. A. H.; Mai, T.
       D.; Kobayashi, M.; Adachi, Y. Adsorptive Removal of Ammonium Ion from
       Aqueous Solution Using Surfactant-Modified Alumina. *Environ. Chem.* **2017**.
       https://doi.org/10.1071/EN17102.

(78)   Padmavathy, V.; Vasudevan, P.; Dhingra, S. C. Thermal and Spectroscopic
       Studies on Sorption of Nickel(II) Ion on Protonated Baker's Yeast.
       Chemosphere **2003**. https://doi.org/10.1016/S0045-6535(03)00222-4.

(79)   Boonamnuayvitaya, V.; Chaiya, C.; Tanthapanichakoon, W. The Preparation
       and Characterization of Activated Carbon from Coffee Residue. *J. Chem. Eng.*
       Japan **2004**. https://doi.org/10.1252/jcej.37.1504.

(80)   Vijaya, Y.; Popuri, S. R.; Boddu, V. M.; Krishnaiah, A. Modified Chitosan
       and Calcium Alginate Biopolymer Sorbents for Removal of Nickel (II)
       through Adsorption. *Carbohydr. Polym.* **2008**.
       https://doi.org/10.1016/j.carbpol.2007.08.010.